

See discussions, stats, and author profiles for this publication at: <https://www.researchgate.net/publication/231272756>

Dimensional Analysis and Scale-up of Immiscible Two-Phase Flow Displacement in Fractured Porous Media under Controlled Gravity Drainage

ARTICLE *in* ENERGY & FUELS · APRIL 2011

Impact Factor: 2.79 · DOI: 10.1021/ef101506n

CITATIONS

22

READS

39

4 AUTHORS, INCLUDING:



Ioannis Chatzis

University of Waterloo

116 PUBLICATIONS 2,580 CITATIONS

[SEE PROFILE](#)



Ali A. Mohsenipour

University of Waterloo

11 PUBLICATIONS 46 CITATIONS

[SEE PROFILE](#)



A. Elkamel

University of Waterloo

306 PUBLICATIONS 2,148 CITATIONS

[SEE PROFILE](#)

Dimensional Analysis and Scale-up of Immiscible Two-Phase Flow Displacement in Fractured Porous Media under Controlled Gravity Drainage

Sohrab Zendehboudi,* Ioannis Chatzis, Ali Asghar Mohsenipour, and Ali Elkamel

Department of Chemical Engineering, University of Waterloo, Waterloo, Ontario N2L 3G1, Canada

ABSTRACT: Oil production from a fractured reservoir, composed of a gas cap and an oil zone, is usually accomplished using surface or submersible pumps. The production method is called controlled gravity drainage (CGD). In the CGD mode of production, the pumps usually operate under a constant withdrawal rate until gas breakthrough, at which time the pumping rate would be influenced by the presence of gas at the production well. In this paper, we describe immiscible displacements in fractured porous media to have a better understanding of the process. Oil–gas CGD displacements were conducted using a laboratory flow apparatus in the fractured glass bead systems. A detailed dimensional analysis was conducted to scale up the experimental results based on the physics of the CGD process and experimental findings. Dimensional analysis of immiscible two-phase flow in porous media allows for quantification of the influences of petrophysical properties of the fractured media and physical properties of test fluids on some important aspects, such as critical pumping rate and recovery factor at gas breakthrough. In this work, an empirical model based on the dimensional groups of the system obtained from the Buckingham π theorem was employed to investigate the gravity drainage process in a fractured porous medium. A model was developed to predict the critical pumping rate, maximum withdrawal rate, distance between the gas–liquid (G–L) interface positions within the matrix and fractures, and recovery factor just before gas breakthrough for fractured porous media undergoing the CGD processes. The model was tested against experimental and field data of oil production under CGD. The results demonstrate that the model gives satisfactory prediction for the oil–gas drainage systems. The procedure outlined in this paper also has potential applications in modeling immiscible displacements.

INTRODUCTION

Gravity drainage is an important production mechanism in the development of many fractured oil reservoirs with attractive characteristics, such as a large dipping angle, significant vertical thickness, and high permeability.^{1–3} The oil production from a fractured porous medium by gravity drainage can be the foundation of a number of industrial processes, such as enhanced oil recovery (EOR) methods and the remediation of polluted groundwater.^{1–3}

In general, the scaling mechanism results in the definition of dimensionless scaling groups. Two general methods for deriving dimensionless numbers can be found in the literature, namely, dimensional analysis and inspectional analysis.^{4–6} Inspectional analysis is established upon the differential equations that govern the physics of the problem, while dimensional analysis is based on knowledge of the significant variables contributing in the process and, in consequence, affecting the response of the system.^{4–6} In inspectional analysis, the differential equations governing the process along with initial and boundary conditions are transformed into dimensionless forms by inserting normalizing variables into the equations. This will lead to dimensionless numbers made of dependent and independent variables and dimensionless similarity or scaling groups.^{4–6}

There are two main reasons to choose dimensional analysis for this study, namely: (1) There are still some uncertainties associated with the term of communication between the matrix and fractures in the continuity equation for fractured media under controlled gravity drainage (CGD); therefore, the formulation of the transfer rate may cause some errors in the prediction of flow behavior. (2) Because we

are dealing with various configurations of fracture networks, it is not easy to normalize the process variables and then derive a general governing equation for all types of fractured porous systems employed in this research.

There is extensive literature on the scaling approach that can be applied to multiphase flow in porous media, such that scaling of miscible and immiscible processes using inspectorial analysis has provided valuable information for a better understanding of the process based on the extracted dimensionless numbers.^{4–10} Leverett et al.⁷ were the first investigators that employed dimensionless groups in the study of immiscible displacements of oil by water in homogeneous oil reservoirs. Engleberts and Klinkenberg⁸ extended their work to figure out important aspects of water flooding in porous media. Croes and Schwarz⁹ presented a comprehensive study to find out the effects of the oil/water viscosity ratio on the recovery performance of water injection as an immiscible displacement process. They introduced a diagram, valid for viscosity ratios between 1 and 500, to provide estimations for cumulative oil production at different operating conditions. However, the diagram is suitable only to homogeneous reservoirs that are following a linear displacement pattern during water injection.⁹ Gratttoni et al.¹⁰ defined a new dimensionless number to include the effects of gravity, viscous, and capillary forces together. This dimensionless group presented a linear relationship with the total recovery for all of the cases tested. Kulkarni and Rao¹¹ investigated the impacts of

Received: November 5, 2010

Revised: March 22, 2011

Published: March 25, 2011

different dimensionless groups on the ultimate oil recovery based on data obtained from various miscible and immiscible gas gravity drainage processes in field and laboratory scales. Wood et al.¹² derived dimensionless groups for tertiary EOR using CO₂ flooding in waterflooded reservoirs and presented screening criteria for EOR methods and storage in the United States Gulf Coast reservoirs.

Scaling-up of experimental data was carried out by Offeringa and van der Poel¹³ for miscible displacement. The first successful attempt was made by Rapoport^{14,15} to employ inspectional analysis in the immiscible displacement of oil by cold water. This research study was later continued by Geertsma et al.¹⁶ to test hot water displacement and solvent flooding for generalizing the previous results. The researchers tried a methodology including a combination of inspectional analysis and dimensional analysis to obtain the dimensionless similarity numbers for these kinds of production methods.¹⁶ In their scaling study, Craig et al.¹⁷ considered anisotropy to investigate the influences of gravity segregation in miscible and immiscible displacements in five-spot models. They found a correlation between the ratio of vertical/horizontal pressure gradient and the oil performance at breakthrough for different mobility ratios. Also, an empirical equation was introduced to correlate the experimental oil recovery versus gravity number for five-spot miscible displacement models.¹⁷ Later on, Perkins and Collins¹⁸ presented scaling criteria that allow for the relative permeability and capillary pressure curves of the model to be different from those of the prototype.¹⁸ van Daalen and van Domslaar¹⁹ employed an inspectional analysis methodology to study scaling-up of models that have different geometries from that of the prototype. They found that, if no cross-flow occurs, then the aspect ratio is not significant in scaling immiscible displacements. However, if cross-flow happens, then the aspect ratio plays an important role in scaling immiscible displacements.¹⁹

Rostami et al.²⁰ studied the forced gravity drainage in homogeneous porous media. They carried out the gravity drainage experiments within wide ranges of the physical properties and operating conditions, such as medium height, permeability, oil viscosity, and gas injection rate. These parameters are altered to obtain a number of dimensionless groups contributing in the forced gravity drainage.²⁰ Although some researchers (e.g., Gharbi et al.⁴ and Grattoni et al.¹⁰) investigated the dimensional and parametric sensitive analysis of gravity drainage, their works dealt with gravity drainage conditions in homogeneous porous media and the issue of fractured porous media remains to be addressed. Hence, it is necessary to investigate the production mechanism and effective parameters for fractured porous media under gravity drainage. Additionally, to the best of our knowledge, no scaling study was performed for the CGD processes.

The current study focuses on CGD, which is pertaining to production with a constant rate during the process. The main attention of this paper is on more complicated porous systems as well as the influencing variables in dimensional analysis, as compared to other works reported in the porous media area. The dimensionless distance between the gas–liquid (G–L) interface positions within the matrix and fractures, “critical pumping rate” (CPR), “maximum possible withdraw rate” (MPWR), and recovery factor at gas breakthrough conditions were correlated as a function of selected dimensionless groups.²¹ In this paper, we focus our attention on the design of a regression analysis procedure that is able to model the response of a process. To do so, one needs “good” estimates of the model parameters; i.e., the contributing parameters should have a minimum amount of statistical variance and should be unbiased in

nature. In other words, if one wishes to design an appropriate regression model, some primary elements should be considered, such as implementing a precise model, logical generalization of modeling results, and quantifying the dependency of response variable(s) on all of the process inputs.^{22,23} In this study, laboratory-scale experiments were performed for validation and physical interpretation of the procedure that we present here.^{21,24–26} A new concept of the CPR was defined. Knowing this particular withdrawal rate offers two main advantages, namely: (1) choosing a pumping rate lower than it to drain the reservoir without having gas breakthrough and (2) understanding the physics of the pumping behavior from fractured media and extending the concept to the real cases. In addition, the maximum liquid pumping rate from each physical model has also been studied, and it was found that this rate strongly depends upon the permeabilities ratio, Bond number, and Reynolds number.^{21,24} The paper also focuses on the scale-up and validation of immiscible displacements in fractured oil porous media using dimensionless groups. The effects of all of the obtained dimensionless scaling groups on important aspects of gravity drainage processes are investigated using a detailed parametric sensitivity and dimensional analysis.

Theory and New Defined Variables. Naturally fractured reservoirs (NFRs) produce over 30% of the world's oil.^{27,31} Pressure-driven oil recovery mechanisms may not be as successful in these types of reservoirs because the fractures create local highly permeable pathways and injected fluids tend to channel toward the production well, reducing the overall recovery efficiency (e.g., issues with flow in dual and triple porosity systems and complex geology).^{1,2,27} Gravity drainage processes are far more effective for economically producing oil from a NFR compared to other methods.^{1,2}

Generally, there are three types of gravity drainage processes:^{3,24–28} (1) When the only driving force is the gravity force without any external force, the displacement process is called free fall gravity drainage (FFGD). The gas tends to penetrate spontaneously into the block by FFGD from the top of the block, and oil is produced from the bottom of the block. Oil is produced only if the gravitational force exceeds the capillary force. The key factors to control the recovery rate and ultimate recovery in a single block are the connate water saturation, oil relative permeability, and matrix capillary pressure.³ (2) Forced gravity drainage in fractured porous media is a process in which gas is injected at the top part of the physical model. In forced gravity drainage, the effectiveness of displacement depends upon not only the relative magnitude of the viscous and gravity forces but also their relative magnitude with respect to the capillary force. In gravity drainage, the gravity force is a driving force, while the capillary force is resistive. Under gas injection, the velocity of the gas front is controlled by the interplay of gravity, capillary, and viscous forces. (3) If oil production from a reservoir with a gas cap and an oil zone takes place at a constant withdrawal rate, the process is called CGD. Interactions between capillary, gravity, and viscous forces affect the production mechanism in the CGD processes significantly. Knowing the effect of the pumping rate on the production performance before gas breakthrough and selecting optimum pumping rates are necessary in managing this type of process better. The cases presented here are similar to porous media models, which are completely saturated with oil, and the reservoir pressure is above or equal to the bubble point pressure of the oil phase. This is the initial condition for the fractured porous systems in this study. Then, the gas is injected to maintain pressure as soon as the production

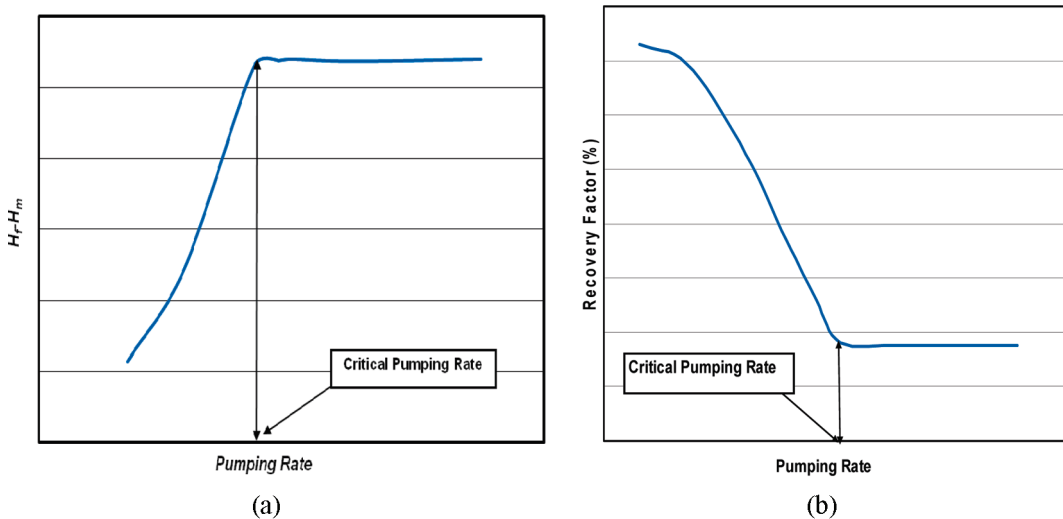


Figure 1. Schematic diagrams of CPR. (a) Relation of CPR to the height difference between the G–L interface positions within fractures and the matrix. (b) Relation of CPR to the recovery factor just before gas breakthrough during the CGD process.

starts, by pumping oil from the medium, and the reservoir pressure drops below the bubble point pressure. As shown in this paper, pressure maintenance helps to sustain a relatively high level of liquid in fractures at initial stages. As another example, suppose that we have a fractured medium with a gas cap and the media is 100% oil-saturated. Now, it is planned to produce from this porous system with a specific constant production rate. Therefore, a ground facility (e.g., a pump) is required to set a certain withdrawal rate. This paper exhibits production behaviors of such examples. Thus, first, we have the liquid level in fractures and the matrix. The liquid level goes down faster, and gas occupies the fractures as the production continues. Finally, matrix blocks are surrounded by the gas phase present in the fractures and gas cap. These models are close to one of Shell's fractured carbonate reservoirs reported in the literature.²⁹ Also, it should be mentioned that the liquid level in the fracture has an important effect on the production mechanism because it helps to establish a strong communication between the matrix and fractures. For example, if fractures are very close to the production well somehow, controlling the withdrawal rate would be vital to manage the liquid level in fractures to have an efficient recovery factor without gas breakthrough from the fractured system.

There are fundamental differences between the recovery factor of fractured and conventional porous media under gravity drainage. Capillarity is the key cause of this diversity. To be more specific, the difference in the capillary pressure of the matrix and fractures has a significant impact on the production performance of fractured oil reservoirs.^{1–3} The recovery of oil by gravity drainage in a fractured reservoir under gas–oil immiscible displacement is less than that in a homogeneous reservoir, clearly. The two mechanisms that affect the gravity drainage performance in a fractured reservoir are^{1–3,28} (1) the capillary pressure contrast between the matrix and the fracture, which causes higher capillary holdup than the non-fractured reservoir, and (2) the reinfiltration process, by which the oil drained from the upper matrix is sucked by the lower matrix. Capillary discontinuity leads to low recovery and reinfiltration causes delay in production.

Before the description of experiments and dimensional analysis parts, it should be noted that there are three characteristic production rates defined throughout this paper that will be presented here first: (1) q_{\max}^{fg} is the maximum production rate of liquid obtained during the FFGD process. This characteristic flow

rate is as follows:³

$$q_{\max}^{\text{fg}} = A \frac{K_e}{\mu_1} \frac{\Delta \rho g(L - h_c)}{L} \quad (1)$$

where q_{\max}^{fg} is the maximum production rate, K_e is the total effective permeability, μ_1 is the viscosity, L is the model height, ρ is the density, g is the gravitational force, and h_c is the capillary threshold height for the porous media. (2) q_{cr} is the CPR of liquids, which is obtained during the CGD process. At this CPR, the elevation difference between the G–L interfaces in the matrix and fractures ($H_f - H_m$) remains constant at a fixed location along the model width, even if the withdrawal rate increases. The ultimate recovery factor, just before gas breakthrough, is unaffected by a further increase in the withdrawal rate beyond this CPR.^{21,24} Figure 1 shows clearly two schematic diagrams for CPR. (3) q_{\max} is the maximum possible withdrawal rate (MPWR) from the models that each particular model can maintain in the porous media during the CGD process. Above this withdrawal rate, the occurrence of viscous fingering and non-wetting phase shortcut toward the production well will eliminate a stable displacement of liquid.^{21,24} At this condition, the viscous force is the dominant force during CGD. This rate robustly depends upon the storage capacity of the fractures, petrophysical properties of each model, and physical properties of test fluids. It should be noted that MPWR is higher than the maximum gravity driven flow rate.

■ EXPERIMENTAL SECTION

Experimental Setup. Figure 2 shows the cartoons of the experimental setups used in the current study. The experimental setups are comprised of the following components (see Figures 2 and 3): (a) a rectangular porous medium, (b) a particular pattern of fractures, (c) high-definition video-recording and high-resolution digital-imaging facilities, (d) peristaltic pump with variable discharge rates, (e) digital balance to weigh the withdrawn liquid, and (f) vacuum equipment to remove dissolved gas from test liquids.

Test Fluids. Varsol oil, deionized water, and aqueous solutions of carboxy methyl cellulose (CMC) with different concentrations were employed as common laboratory liquids for investigating the oil recovery history and G–L interface movements by CGD, primarily in

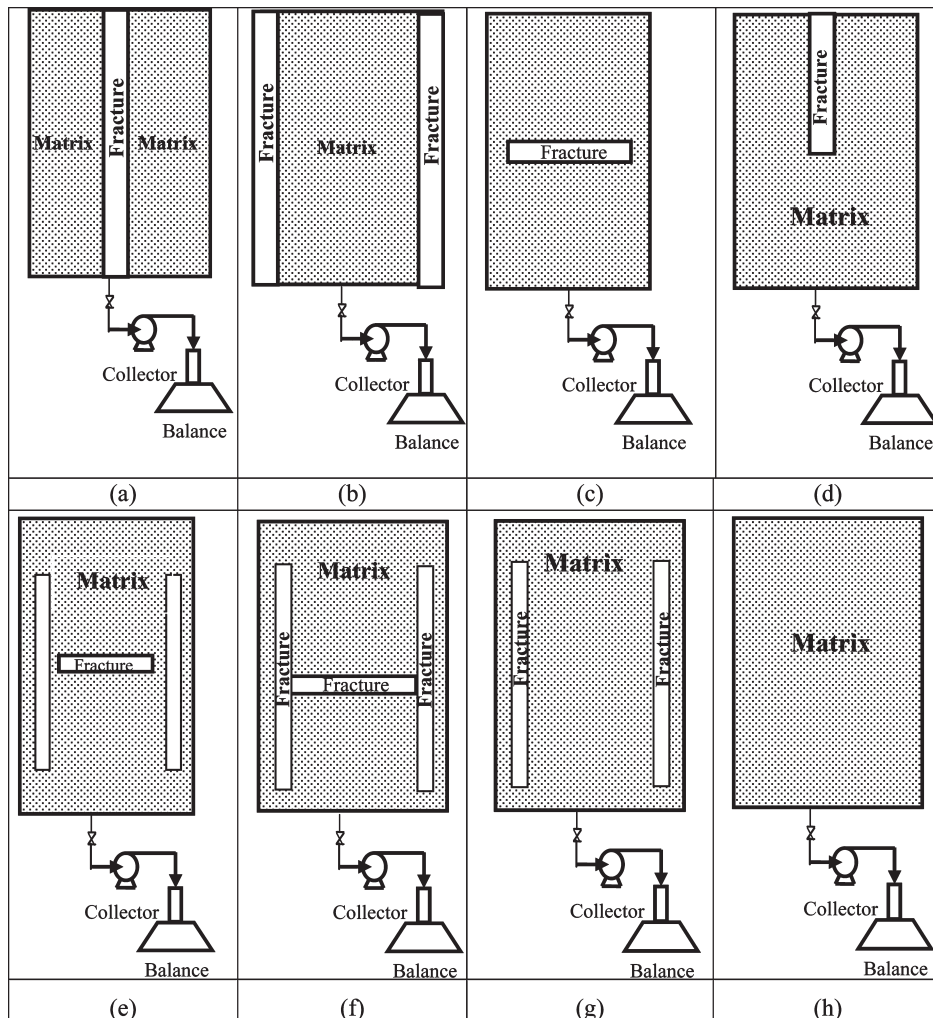


Figure 2. Cartoons of the apparatus used for CGD in porous media with various patterns of fractures.

fully saturated porous media models. Water viscosity was increased by adding CMC to represent different oil viscosities. The physical properties of the fluids are listed in Table 1.

Experimental Methodology. CGD experiments were conducted at room conditions. The porous media models with fractures were of rectangular geometry, with certain patterns of fracture arrangement. The test fluids were first deaerated to avoid developing non-wetting phase saturation within the porous medium. Then, a known volume of liquid was filled into the fractured model. Glass beads were loaded from the top of the model while packing continuously. The packing operation must be continuous to prevent the formation of any layering of fine particles in the fractured medium during the packing process. The loading of glass beads was stopped when the glass beads in the rectangular model reached 1–2 cm above the target height. After 5 min of tapping the physical model with a hammer, the height of the glass beads would continuously drop. After that, more glass beads were added to the fractured porous medium to achieve the target height. Every time glass beads were added, manual mixing with a stick was needed to ensure packing uniformity at the top section of the packing. After the packing, the possible extra liquid above the packing was drained out and excluded from the initial pore volume of liquid in the model.

The saturated packed model was then used for gravity drainage experiments. Figure 3 shows a schematic of the CGD process in more detail. A peristaltic pump was used to withdraw the liquid from the fractured and homogeneous models at various fixed flow rates; a wide

range of pumping rates was applied to each particular fractured medium during the CGD experiments to find CPR and MPWR. The peristaltic pump was connected to the bottom horizontal well (shown by the diagonal pinstripe pattern in Figure 3) to avoid resistance-to-flow on the production side. The production of the liquid phase from the models was collected and weighed on a cumulative basis as a function of the time, using a digital balance. A high-resolution camcorder was employed for continuous recording of the liquid–air interface positions during the gravity drainage experiments in the matrix and in the fractures. Pictures taken at various stages of gravity-stabilized displacement were analyzed for tracking the G–L interface advancement through the matrix and fractures. G–L interface positions in both the matrix and fractures “ $H(t)$ ” were measured from the top portion of each individual packing all of the way down along the height of the model with respect to time as the gas phase invaded the fractures and matrix space, respectively. In some experiments, we added an oil-soluble dye to Varsol oil to enhance the visibility of oil flow pathways through the model.

Experimental Data Collection and Analysis Approach. CGD experiments were carried out in various models with different initial conditions. The experiments have been repeated 2 or 3 times to double check accuracy. For each run, the average results were considered to obtain both the production history and the G–L interface advancement in the matrix and fractures. Looking at the replicate runs preformed in this study shows clearly that almost all of the performed experiments were conducted as accurately as possible; i.e., a high degree of

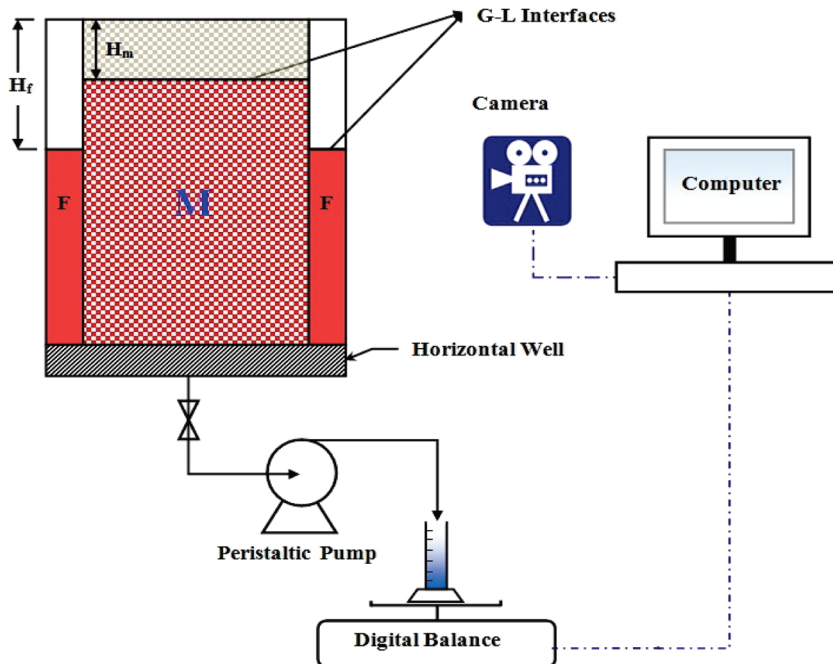


Figure 3. Schematic of the CGD experiments in fractured models.

Table 1. Physical Properties of Test Fluids

test fluid	density (g/cm ³)	surface tension (mN/m)	viscosity (mPa s)
CMC solution (1%)	1.05	73.23 ± 0.6	4.80 ± 0.3
CMC solution (2%)	1.07	74.15 ± 0.5	11.91 ± 0.4
Varsol oil	0.78	25.04 ± 0.5	1.22 ± 0.3
water	1.00	72.02 ± 0.4	1.01 ± 0.2
air	1.20 × 10 ⁻³	N/A	1.80 × 10 ⁻²

repeatability was achieved (refer to Table A1 in the Appendix). A summary of model characteristics is presented in Table 2. Experimental results related to 27 sample experiments are presented in Table 3.

A parametric sensitivity analysis was performed to investigate the effect of different parameters on some aspects of the CGD process, such as the newly defined concepts of CPR and MPWR. The effects of model height, matrix permeability, fluid pair properties, and fracture aperture on the CGD process performance were investigated. This analysis contains both quantitative (i.e., analyzing the drainage rates, cumulative production versus time, and investigating CPR and MPWR at different conditions) and qualitative (i.e., analysis of interface movements in both fractures and matrix using video-recording and digital-imaging techniques) approaches. The experimental results were published by Zendebsoudi et al.^{24–26,30} elsewhere. Hence, because of the limitations in the length of technical papers and also avoiding unnecessary overlap between publications, we found it better to make this part brief in this paper. To provide technical readers with further details, we presented briefly the main results of parametric sensitivity analyses through the paper. In addition, this part helps the readers follow the dimensional analysis introduced here easier.

BRIEF OF PARAMETRIC SENSITIVITY ANALYSIS

As explained previously, a parametric sensitivity analysis has been performed on the fractured porous media under CGD and was published recently elsewhere.^{24,25} This section presents a brief of the results of the work to clarify more physical concepts of

CGD and multivariable regression analysis. (1) The experimental data show that, as long as the pumping rate is constant, the elevation difference between the G–L interface positions in both the matrix and fracture parts of media remains unchanged during each particular CGD experiment. In addition, when the liquid withdrawal rate is increased, considering all other system parameters remain unchanged, the rate of the G–L interface recession in both the matrix and fractures increases as well. This increase in the recession rate of the G–L interface also increases the elevation difference between the G–L interface positions within the matrix and fractures ($H_f - H_m$). (2) Effect of the model height: At each particular fixed drainage rate, taller models have the ability to maintain that particular withdrawal rate for a longer duration of time, which leads into a higher recovery factor before gas breakthrough. Also, the taller the model, the higher its associated CPR and MPWR if other contributing properties are kept the same for all porous models under CGD. (3) Effect of the fracture aperture (or fracture permeability): Because models with a larger fracture aperture have a higher fracture storage capacity, therefore, under similar circumstances of the CGD type of process, they should have higher recovery factor values at gas breakthrough. Moreover, it was concluded that models with a larger fracture aperture show higher CPR and MPWR values. (4) Effect of the matrix permeability: It is clear that the higher the matrix permeability value, the higher the associated cumulative production, as well as the recovery factor, when all other

Table 2. Properties of Employed Packed Models

run number	fracture height, L_f (cm)	matrix glass bead type	porosity (%)			permeability (darcy)		viscosity (mPa s)	fracture aperture, "b" (mm)	fracture pattern	well location
			ϕ_f	ϕ_m	ϕ_e	K_{ef}	K_m				
1	55	BT2	1.41	38	38.86	15979	1013	4.8 ± 0.3	5	b	center
2	55	BT2	1.41	38	38.86	15979	1013	11.9 ± 0.4	5	b	center
3	55	BT2	1.41	38	38.86	15979	1013	11.9 ± 0.4	5	b	corner
4	55	BT2	1.41	38	38.86	15979	1013	1.0 ± 0.2	5	b	center
5	55	BT2	0.92	38	38.56	3465	1013	11.9 ± 0.4	3	b	center
6	55	BT2	0.92	38	38.56	3465	1013	4.8 ± 0.3	3	b	center
7	55	BT3	1.41	38	38.86	15979	408	4.8 ± 0.3	5	b	center
8	55	BT3	1.41	38	38.86	15979	408	11.9 ± 0.4	5	b	center
9	55	BT3	1.41	38	38.86	15979	408	11.9 ± 0.4	5	b	corner
10	28	BT3	1.41	38	38.86	15979	408	11.9 ± 0.4	5	b	center
11	40	BT3	1.41	38	38.86	15979	408	11.9 ± 0.4	5	b	center
12	55	BT4	1.41	38	38.86	15979	204	4.8 ± 0.3	5	b	center
13	55	BT3	1.41	38	38.86	15979	408	1.0 ± 0.2	5	b	center
14	55	BT4	1.41	38	38.86	15979	204	11.9 ± 0.4	5	b	center
15	55	BT4	1.41	38	38.86	15979	204	11.9 ± 0.4	5	b	corner
16	55	BT4	0.92	38	38.56	3465	204	4.8 ± 0.3	3	b	center
17	55	BT4	1.41	38	38.86	15979	204	1.0 ± 0.2	5	b	center
18	55	BT2	0.62	38	38.37	1028	1013	11.9 ± 0.4	2	b	center
19	55	BT2	0.62	38	38.37	1028	1013	11.9 ± 0.4	2	b	corner
20	55	BT3	1.41	38	38.86	15979	408	1.2 ± 0.3	5	b	center
21	55	BT3	0.70	38	38.43	7989	408	1.2 ± 0.3	5	a	center
22	55	BT3	0.23	38	38.14	2619	408	1.2 ± 0.3	5	c	center
23	55	BT3	0.35	38	38.23	4000	408	1.2 ± 0.3	5	d	center
24	55	BT3	1.41	38	38.86	15979	408	1.2 ± 0.3	5	e	center
25	55	BT3	1.53	38	38.86	17120	408	1.2 ± 0.3	5	f	center
26	55	BT3	1.21	38	38.74	13696	408	1.2 ± 0.3	5	g	center
27	55	BT3	N/A	38	38.00	N/A	408	1.2 ± 0.3	5	h	center

parameters remain unchanged. Another important result is that both of these system-specific drainage rates, CPR and MPWR, increase almost linearly when the matrix permeability increases. (5) Effect of the liquid viscosity: At a constant withdrawal rate, it was found that, the higher the liquid viscosity, the lower its associated recovery factor. Also, we concluded that both CPR and MPWR decrease as a result of an increase in the liquid viscosity. (6) Effect of the liquid interfacial tension (IFT): Low IFT values improve the final recovery because of increased gravity effects. IFT has significant effects on CPR and MPWR because both specific drainage rates will increase if the value of this liquid property decreases.

DIMENSIONLESS GROUPS

In this section, the relevant dimensionless groups that play important roles in the upscaling of the experimental results are discussed accordingly. The Buckingham π theorem was applied to produce dimensionless groups. The number of variables depends upon response variables. According to the experimental studies, Table 4 shows all possible variables in the current study. Also, all of the possible dimensionless groups are listed in Table 5.

It should be noted here that the variability of some parameters (i.e., thickness and width) was not considered in the current study. This is mainly due to the fact that results from the experimental work revealed that only nine parameters are important variables to be

considered in this study. This means that the number of dimensionless groups on the basis of the Buckingham π analysis, would be six, including RF, $(K_m \Delta \rho g)/\sigma$, $L/\Delta h$, K_f/K_m , $(\mu_l V)/\sigma$, and $(\rho_l V D_p)/\mu_l$.

Consequently, six dependent variables are taken into consideration as significant dimensional variables for the recovery factor at gas breakthrough and the elevation difference between the G–L interface positions in the matrix and fractures, according to the above table. Five dependent variables are also considered as effective parameters that affect the magnitude of CPR and MPWR.

Capillary Number. In fluid dynamics, the capillary number represents the relative magnitude of viscous forces to the capillary forces acting across a particular interface between a liquid and gas phase or between two immiscible liquid phases.³ The capillary number is defined as

$$Ca = \frac{\mu_l V}{\sigma} \quad (2)$$

where " μ_l " is the liquid viscosity, "V" is the withdrawal velocity in this work, and " σ " is the surface or IFT between the two fluid phases. As a rule of thumb,^{3,31} one can consider the fluid flow in a porous medium to be dominated mainly by capillary forces if the associated value of the capillary number is equal to or less than 10^{-5} . The liquid viscosity and withdrawal rate profoundly affect the recovery factor and the G–L interface locations within the matrix and fractures. When the capillary number is defined as one

Table 3. Results of CGD Experiments for 27 Sample Runs

run number	model height, <i>L</i> (cm)	matrix glass bead type	fracture aperture, “ <i>b</i> ” (mm)	viscosity, “ μ_l ” (mPa s)	recovery factor (% PV)	fracture pattern	S_{or} (% PV)	CPR, ^a “ q_{cr} ” (cm ³ /s)	MPWR, ^b q_{max} (cm ³ /s)
1	55	BT2	5	4.8 ± 0.3	85.2 ± 0.5	b	16.1 ± 0.5	8.6 ± 0.1	8.9 ± 0.2
2	55	BT2	5	11.9 ± 0.4	85.2 ± 0.3	b	16.2 ± 0.3	4.3 ± 0.3	7.1 ± 0.3
3	55	BT2	5	11.9 ± 0.4	85.1 ± 0.4	b	16.1 ± 0.2	3.8 ± 0.2	4.9 ± 0.2
4	55	BT2	5	1.0 ± 0.2	85.2 ± 0.2	b	16.2 ± 0.1	9.4 ± 0.2	11.4 ± 0.1
5	55	BT2	3	11.9 ± 0.4	85.3 ± 0.4	b	16.3 ± 0.1	4.0 ± 0.3	5.9 ± 0.2
6	55	BT2	3	4.8 ± 0.3	85.0 ± 0.3	b	16.1 ± 0.4	7.5 ± 0.1	7.8 ± 0.2
7	55	BT3	5	4.8 ± 0.3	83.0 ± 0.4	b	18.2 ± 0.3	3.1 ± 0.2	6.1 ± 0.1
8	55	BT3	5	11.9 ± 0.4	83.2 ± 0.5	b	18.3 ± 0.2	1.5 ± 0.3	5.4 ± 0.3
9	55	BT3	5	11.9 ± 0.4	83.1 ± 0.2	b	18.1 ± 0.3	1.3 ± 0.2	4.4 ± 0.1
10	28	BT3	5	11.9 ± 0.4	83.0 ± 0.4	b	18.2 ± 0.2	0.8 ± 0.1	3.8 ± 0.3
11	40	BT3	5	11.9 ± 0.4	83.1 ± 0.4	b	18.1 ± 0.3	1.1 ± 0.3	4.4 ± 0.3
12	55	BT4	5	4.8 ± 0.3	81.2 ± 0.2	b	20.2 ± 0.1	1.4 ± 0.2	5.1 ± 0.2
13	55	BT3	5	1.0 ± 0.2	83.1 ± 0.5	b	18.1 ± 0.2	6.6 ± 0.2	7.5 ± 0.2
14	55	BT4	5	11.9 ± 0.4	81.2 ± 0.3	b	20.0 ± 0.3	0.7 ± 0.3	4.8 ± 0.1
15	55	BT4	5	11.9 ± 0.4	81.2 ± 0.1	b	20.1 ± 0.2	0.5 ± 0.2	4.0 ± 0.1
16	55	BT4	3	4.8 ± 0.3	81.3 ± 0.3	b	20.2 ± 0.2	1.2 ± 0.3	4.3 ± 0.1
17	55	BT4	5	1.0 ± 0.2	81.2 ± 0.4	b	20.1 ± 0.1	3.3 ± 0.1	5.7 ± 0.2
18	55	BT2	2	11.9 ± 0.4	85.3 ± 0.4	b	16.0 ± 0.3	3.4 ± 0.1	4.9 ± 0.2
19	55	BT2	2	11.9 ± 0.4	85.2 ± 0.3	b	16.2 ± 0.2	3.1 ± 0.2	4.1 ± 0.3
20	55	BT3	5	1.2 ± 0.3	84.3 ± 0.4	b	17.1 ± 0.5	6.4 ± 0.3	7.3 ± 0.2
21	55	BT3	5	1.2 ± 0.3	84.2 ± 0.1	a	17.2 ± 0.4	6.2 ± 0.3	7.0 ± 0.1
22	55	BT3	5	1.2 ± 0.3	84.5 ± 0.3	c	17.2 ± 0.3	N/A	5.2 ± 0.3
23	55	BT3	5	1.2 ± 0.3	84.4 ± 0.5	d	17.0 ± 0.3	4.9 ± 0.3	5.9 ± 0.3
24	55	BT3	5	1.2 ± 0.3	84.2 ± 0.4	e	17.3 ± 0.1	7.0 ± 0.1	8.2 ± 0.2
25	55	BT3	5	1.2 ± 0.3	84.1 ± 0.3	f	17.1 ± 0.2	7.2 ± 0.2	8.4 ± 0.1
26	55	BT3	5	1.2 ± 0.3	84.2 ± 0.2	g	17.2 ± 0.1	6.2 ± 0.3	7.1 ± 0.2
27	55	BT3	5	1.2 ± 0.3	84.1 ± 0.4	h	17.1 ± 0.1	N/A	5.0 ± 0.3

^a CPR = critical pumping rate. ^b MPWR = maximum possible withdrawal rate.Table 4. Dependent and Independent Variables Used for the Buckingham π Theorem

variable	dimension	variable	dimension
particle diameter (D_p)	$M^0 L^1 T^0$	matrix porosity (ϕ_m)	$M^0 L^0 T^0$
liquid density (ρ_l)	$M^1 L^{-3} T^0$	G–L surface tension (σ)	$M^1 L^1 T^{-2}$
gas density (ρ_g)	$M^1 L^{-3} T^0$	withdrawal velocity (V)	$M^0 L^1 T^{-1}$
matrix permeability (K_m)	$M^0 L^2 T^0$	fracture aperture (b)	$M^0 L^1 T^0$
fracture permeability (K_f)	$M^0 L^2 T^0$	gravitational force (g)	$M^0 L^1 T^{-2}$
liquid viscosity (μ_l)	$M^1 L^{-1} T^{-1}$	matrix width (W)	$M^0 L^1 T^0$
gas viscosity (μ_g)	$M^1 L^{-1} T^{-1}$	position difference between the G–L interface in the matrix and fracture (Δh)	$M^0 L^1 T^0$
model height (L)	$M^0 L^1 T^0$	recovery factor (RF)	$M^0 L^0 T^0$
fracture porosity (ϕ_f)	$M^0 L^0 T^0$		

of the contributing dimensionless groups in the regression analysis, one could realize the importance of these two independent variables on the statistical modeling response.

Bond Number. The Bond number, Bo , is a dimensionless number expressing the ratio of body forces (often gravitational) to capillary forces^{3,28}

$$Bo = \frac{\Delta \rho g l^2}{\sigma} \quad (3)$$

where “ $\Delta \rho$ ” is the density difference between two fluids, “ g ” is the acceleration due to gravity, “ l ” is a characteristic length (often taken

as the average grain diameter³), and “ σ ” is the surface or IFT. In this study, we used (K_m) instead of (l^2) in the Bond number expression.

For a vertical displacement, Bo represents the balance between gravity and capillary forces and is directly proportional to the velocity of the displacing phase front. Thus, Bo can also be a dynamic parameter additionally depending upon the front velocity. Because knowledge of the Bond number value is essential for investigating different aspects of either the free or forced gravity drainage process, it is wise to consider it as one of the reference dimensionless groups. This makes it possible to realize its physical importance on the different aspects of the

Table 5. Dimensionless Groups Obtained Using the Buckingham π Analysis

dimensionless group	definition
ρ_l/ρ_g	ratio of liquid density/gas density
W/L	ratio of model width/model height
ϕ_f/ϕ_m	ratio of fracture porosity/matrix porosity
$Bo = (K_m \Delta \rho g)/\sigma$	Bond number (Bo) based on matrix permeability; ratio of gravitational force/surface tension force
$Fr_{PM} = V^2/(g(K_m)^{1/2})$	Froude number (Fr_{PM}) in porous media; ratio of inertial force/gravitational force
RF	recovery factor; ratio of the amount of recovered oil/total oil in place
$L/\Delta h$	model height to the elevation difference between the G–L interface positions within the matrix and fractures as a dimensionless height
μ_o/μ_g	ratio of oil (liquid) phase/gas phase
b/L	ratio of fracture aperture/model height
K_f/K_m	ratio of fracture permeability/matrix permeability
$Ca = (\mu_l V)/\sigma$	capillary number (Ca); ratio of viscous force/surface tension force
$Re = (\rho_l V D_p)/\mu_l$	Reynolds number (Re) in porous media; ratio of inertial force/viscous force
ϕ_m	matrix porosity
$Ar = (gL^3 \rho_l^2)/\mu_l^2$	Archimedes number (Ar); ratio of gravitational force/viscous force

CGD process, including CPR, MPWR, and elevation difference between G–L interface positions in the matrix and fractures.

Reynolds Number. Because of the belief that non-Darcy flow in porous media is similar to turbulent flow in a conduit, the Reynolds number for identifying turbulent flow in conduits was adapted to describe non-Darcy flow in porous media.^{3,28} For fluid flow experiments in packed particles, the Reynolds number, Re , is defined as

$$Re_p = \frac{\rho V D_p}{\mu} \quad (4)$$

where D_p is the average particle diameter. Darcy's law is valid as long as the Reynolds number based on the average grain diameter does not exceed some value between 1 and 10. Experimental studies in porous media have suggested that the critical Reynolds number for non-Darcy flow to become significant is in the range of 40–80.^{3,28} To be consistent with the majority of literature cases in which this dimensionless number has been defined, a macroscopic discharge velocity (i.e., withdrawal rate in the case of flow under the gravity drainage process) was used in our analogy regarding dimensionless analysis of the CGD process.^{3,24}

Ratio of Fracture Permeability/Matrix Permeability (K_f/K_m). The K_f/K_m ratio is the main factor affecting fluid flow in both the matrix and fractures during the course of the CGD process. It would be beneficial if one could consider the importance of this ratio in the dimensionless analysis. Because the medium permeability (either matrix or fracture) contributes significantly to the flow potential, the ratio of the fracture permeability/matrix permeability represents the flow potential contrast between these two flow-related media. In addition, the contrast between the fracture and matrix permeabilities also encourages liquid flow exchange between these two media. Moreover, it has a profound effect on the final recovery factor values as well as the amount of gas invasion into the matrix. As a result, this dimensionless parameter was considered as one of the groups required for the dimensionless analysis of the CGD process performance.

Dimensionless Height ($L/\Delta h$). To fulfill the sufficient numbers of dimensionless groups required for the dimensionless analysis, the dimensionless height was defined as the ratio of the magnitude of the model height, " L " (which is constant for each particular packing height) to the magnitude of the elevation difference between G–L interface positions within the matrix

and fractures, " Δh ", in each particular fractured medium. The latter is dictated by the value of the withdrawal rate, which was set for each particular CGD process. The main reason for defining this dimensionless parameter is to figure out how the height difference between liquid level positions within fractures and the matrix would be influenced by changing the main independent parameters noted in CGD experiments.

Recovery Factor (RF). Commonly used in reservoir engineering, this dimensionless parameter may be defined as the ratio of produced oil/oil in place in a reservoir. It is accepted that recovery factor estimation is a tool for rapid assessment of suitability of recovery methods at given conditions. To ease evaluation, the results are ranked by the value of recovery factor.

Multiple Linear Regression Models. In many applications of regression analysis, it is common that there is more than one regressor variable. A regression model that contains more than one regressor variable is called a multiple regression model.^{22,23} As described in the previous section, the proposed dimensionless analysis contains six dimensionless groups, namely: Bo , Ca , Re , (K_f/K_m) , $(L/\Delta h)$, and RF. The next step is to establish the regression models to relate the objective parameters to the dimensionless groups mentioned above. In this study, four such variables for each CGD experiment are considered, namely: CPR, MPWR, RF, and the elevation difference between G–L interface positions within fractures and the matrix. These four response variables should be statistically described as functions of the defined dimensionless groups. To perform the multiple linear regression analysis, these four objective functions should be expressed explicitly in the dimensionless form.

Both, the CPR and MPWR could be related to the drainage liquid velocity or liquid volumetric flow rate and could be expressed in terms of the capillary number. Hence, two corresponding capillary numbers were defined: the critical capillary number, associated with the CPR, and the maximum capillary number, associated with the MPWR. Recalling the definition of the capillary number, the critical capillary number would be the ratio of viscous forces associated with the critical pumping velocity (or CPR) to the capillary forces applied across the G–L interface. Similarly, the maximum capillary number is also defined as the viscous forces associated with the MPWR, divided by the capillary forces associated with the G–L interface. As a result, these two important parameters (CPR and MPWR) or

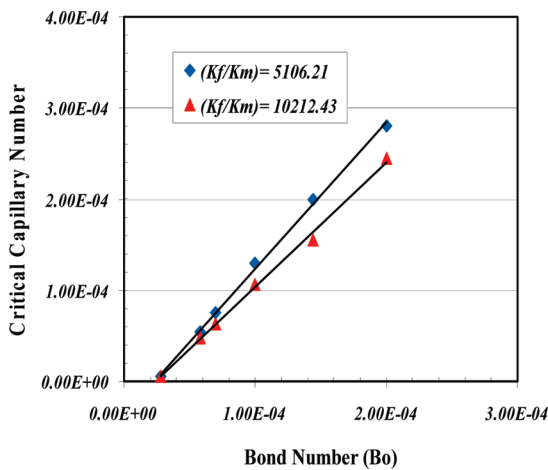


Figure 4. Effect of the Bond number (Bo) on the critical capillary number to find the critical flow rate during controlled gravity draining at various conditions.

their equivalent dimensionless groups (critical capillary number or dimensionless CPR and maximum capillary number or dimensionless MPWR) could be estimated statistically in terms of the other mentioned dimensionless groups. The “recovery factor” response variable is dimensionless. The elevation difference between G–L interface positions within the matrix and fractures would also be altered to the dimensionless form by introducing the “dimensionless height” group. In other words, the height of each particular physical model divided by the elevation difference between interface positions within the matrix and fractures forms this dimensionless objective function.

To perform the multiple linear regression analysis and to figure out the dependency of a particular dimensionless response variable upon a particular dimensionless group, scatter plots should be prepared. Such plots will illustrate the absolute effect of each of the dimensionless groups [capillary number, Bond number, Reynolds number, and (K_f/K_m)] on the dimensionless response variables. We note that such analysis first assumes no interaction term between the defined dimensionless predictor variables. In this case, a resulting correlation would have the following form:^{22,23}

$$y = \beta_0 + \beta_1 x_1 + \beta_2 x_2 + \dots + \beta_k x_k + e \quad (5)$$

The above relation represents a multiple linear regression model, with “ k ” regressor variables (x_1 – x_k).^{22,23} For the parameters, “ β_0 – β_k ” are called the regression coefficients, x_1 , x_2 , ..., x_k are the dimensionless numbers, and “ y ” is the actual response variable.^{22,23} Interaction terms should also be investigated to predict the flow behavior of porous media under gravity drainage processes. For the case of “ k ” regressor variables, the model relating the regressors to the response, y_i , is as follows:

$$\begin{aligned} y_i &= \beta_0 + \beta_1 x_{i1} + \beta_2 x_{i2} + \dots + \beta_k x_{ik} + e_i \\ i &= 1, 2, \dots, n \end{aligned} \quad (6)$$

For n observations (experimental measurements), this model could be represented as a system of “ n ” equations and is expressed in the matrix notation^{22,23} as

$$y = X\beta + e \quad (7)$$

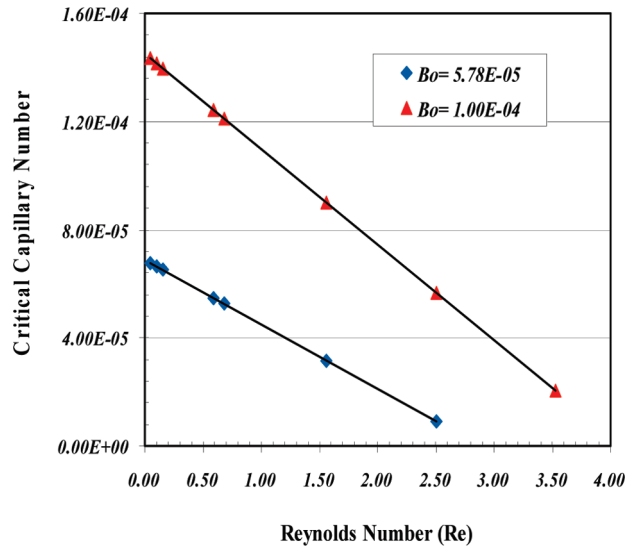


Figure 5. Linear function of the critical capillary number with respect to Reynolds number, while the fractured porous media are under CGD.

where

$$\begin{aligned} y &= \begin{bmatrix} y_1 \\ y_2 \\ \vdots \\ y_n \end{bmatrix}, X = \begin{bmatrix} 1 & x_{11} & x_{12} & \cdots & x_{1k} \\ 1 & x_{21} & x_{22} & \cdots & x_{2k} \\ \vdots & \vdots & \vdots & & \vdots \\ 1 & x_{n1} & x_{n2} & \cdots & x_{nk} \end{bmatrix}, \\ \beta &= \begin{bmatrix} \beta_0 \\ \beta_1 \\ \vdots \\ \beta_k \end{bmatrix}, \text{ and } e = \begin{bmatrix} e_1 \\ e_2 \\ \vdots \\ e_n \end{bmatrix} \end{aligned} \quad (8)$$

The least-squares estimate of the “ β ” parameter can be found^{22,23} as

$$\hat{\beta} = (X'X)^{-1}X'y \quad (9)$$

On the basis of the physics of the CGD process published by Zendehboudi et al.,^{24–26,30} it is found that the combination of dependent dimensionless groups also has a major contribution in the magnitudes of all of the objective functions. As a result, regression models should include the terms related to the “effect of the interaction between the dependent dimensionless groups” as well. An interaction between two dependent variables can be represented by a cross-product term in the regression model, such as

$$y = \beta_0 + \beta_1 x_1 + \beta_2 x_2 + \beta_{12} x_1 x_2 + e \quad (10)$$

To clarify the method of dimensional analysis for technical readers, we illustrate the procedure of a multiple regression model for the critical capillary number, which is in fact related to the CPR.

After the results are obtained from the experiments for CPR, MPWR, RF, and $(\Delta h = H_f - H_m)$, they are substituted in the equations of associated dimensionless numbers to perform a parametric sensitivity analysis. For example, the procedure to plot Figures 4–6 and then obtain eq 12 is as follows: (1) According to the Buckingham π analysis and physical concepts of CGD, we know that the response variable (CPR) is a function of Bo , Re , and K_f/K_m . (2) In the first step, the critical capillary number ($Ca_{cr} = (V_{cr} u_l)/\sigma$) is calculated on the basis of

physical properties of test fluids given in Table 2 and the CPR obtained from the experiment (see Table 3) for a certain run performed on a particular physical model. (3) Then, the Bond number ($Bo = (\Delta \rho g K_m)/\sigma$) of the same run test is obtained by plugging physical properties of test fluid and matrix permeability in the Bond number equation. (4) Steps 2 and 3 are continued for all of the runs that have an identical permeability ratio. (5) Then, we can plot Ca_{cr} versus Bo for two different but constant ratios of fracture permeability/matrix permeability of the fractured porous systems (see Figure 4). (6) The same procedure is applied to have other figures for this scale-up investigation. (7) When all figures for CPR are plotted, we find a general correlation for CPR versus dependent dimensionless numbers with unknown coefficients of contributing terms. (8) Using eqs 6–9, the coefficients of the dimensionless groups existing in the associated regression correlation are calculated. The easier way is to employ Microsoft Excel along with MATLAB software to compute the coefficients.

This algorithm is used for other response variables, such as RF and MPWR.

Multiple Linear Regression Analysis for the Critical Capillary Number. Figures 4–6 are cross-plots showing the effects of different dimensionless groups (namely, K_f/K_m , Bond number, and critical Reynolds number) on the critical capillary number. The critical capillary number was first expressed as a function of the dependent dimensionless variables according to the following relationship:^{22,23}

$$Ca_{cr} = \frac{V_{cr}\mu_l}{\sigma} = f_1 \left(Bo, Re_{cr}, \frac{K_f}{K_m}, \text{combination of these numbers} \right)$$

$$\text{and } Re_{cr} = \frac{\rho V_{cr} D_p}{\mu_l} \quad (11)$$

in which “ V_{cr} ” is the critical velocity associated with the CPR for each particular CGD experimental run.

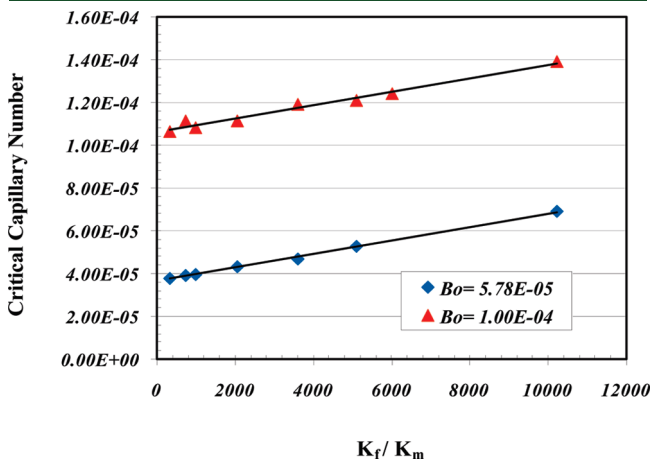


Figure 6. Influence of K_f/K_m on the critical capillary number for two different values of the Bond number.

Table 6. Information Table for the Linear Regression Model of the Critical Capillary Number ($R^2 = 0.997$; $F = 4.78027 \times 10^2$)

coefficients	numerical value	standard error	lower 95%	upper 95%
a	-5.15397×10^{-5}	1.28711×10^{-5}	-8.02182×10^{-5}	-2.28614×10^{-5}
b	18.06884×10^{-1}	9.12360×10^{-2}	16.03598×10^{-1}	20.10169×10^{-1}
c	-8.43132×10^{-6}	9.15642×10^{-6}	-28.83312×10^{-6}	-1.19705×10^{-5}
d	3.12541×10^{-9}	1.26261×10^{-9}	3.12108×10^{-10}	5.93868×10^{-9}
e	-2.69152×10^{-1}	7.23550×10^{-2}	-4.30370×10^{-1}	-1.07934×10^{-1}

Figures 4–6 show that the critical capillary number increases linearly with an increase of both the Bond number and K_f/K_m and decreases linearly with an increase of the critical Reynolds number. As the liquid viscosity increases, the CPR increases as well. As the fracture permeability (i.e., fracture aperture) increases (or “ K_f/K_m ” increases), then the fractured system is capable of handling higher magnitudes of liquid withdrawal velocity (i.e., higher associated CPRs). The last term in eq 12 represents the interaction effect of dependent dimensionless groups on the magnitude of dimensionless CPR. Figures 4–6 show that this interaction term consists of two dimensionless groups, namely, the Bond number and critical Reynolds number; therefore, eq 11 could be rewritten as

$$Ca_{cr} = \frac{V_{cr}\mu_l}{\sigma} = a + bBo + cRe_{cr} + d \frac{K_f}{K_m} + e\{BoRe_{cr}\} \quad (12)$$

Table 6 provides the information regarding the correlation coefficients of eq 12, standard errors, and lower limits as well as upper limits of the coefficients.

The critical withdrawal velocity (which is associated with CPR) appears at both sides of eq 12. As a result, to obtain the CPR for any particular fractured setup, one needs to apply an iterative root finding technique. As an initial guess for the iterative procedure, considering the critical Reynolds number to be equal to unity would be a reasonable trial. The critical withdrawal velocity associated with $Re_{cr} = 1.0$ guarantees a Darcian flow, by which the iterative procedure could be initiated. Knowing the initial guess for “ $V_{cr, \text{guessed}}$ ”, the right-hand side of eq 12 could be solved because all of the parameters are known based on the information provided for each particular CGD experiment. Consequently, the first calculated critical capillary number would be obtained, and as a result, the associated “ $V_{cr, \text{calculated}}$ ” could be obtained. If the calculated critical withdrawal velocity would not be similar to its guessed value (i.e., its associated relative error would not be within a reasonable domain), the “ $V_{cr, \text{calculated}}$ ” would be considered as the second guessed value and the iterative procedure would be repeated accordingly, until a reasonable match between calculated and guessed values of the critical withdrawal velocity would be obtained.

Multiple Linear Regression Analysis for the Maximum Capillary Number. From the experimental investigation of the CGD process, it was concluded that there is a maximum withdrawal rate (i.e., maximum macroscopic drainage velocity) for each particular fractured media under the CGD process, below which a constant withdrawal rate could be maintained for a reasonable duration of time. Practically, it is viable to drain a fractured system at a rate below the maximum withdrawal rate. As a result, determining the maximum drainage rate for each particular fractured porous medium undergoing a CGD process is a necessity to evaluate the performance of this recovery technique.

The multiple linear regression analysis could be implemented to figure out the dimensionless groups affecting the maximum

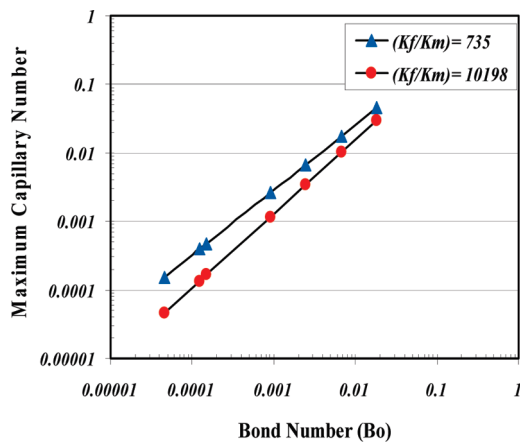


Figure 7. Effect of the Bond number on the maximum capillary number, “ Ca_{\max} ”, for two different values of K_f/K_m .

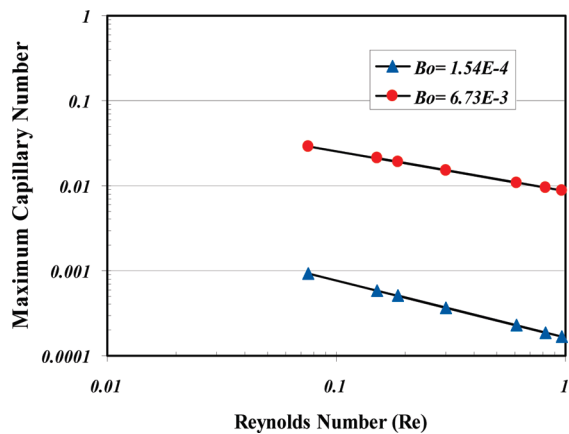


Figure 9. Effect of “ Re ” on “ Ca_{\max} ” at two different values of the Bond number.

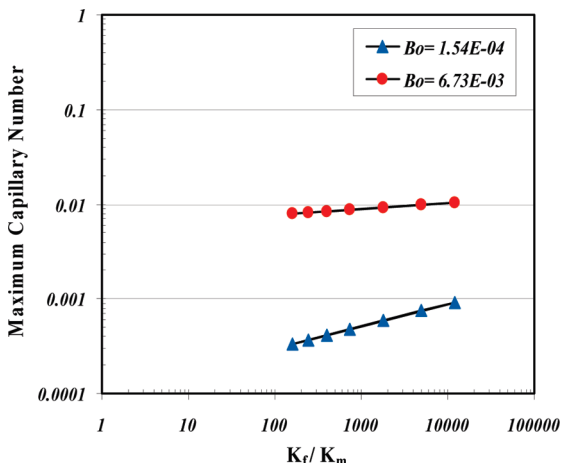


Figure 8. Maximum capillary number, “ Ca_{\max} ”, versus the permeability ratio in a logarithmic plot.

withdrawal rate associated with each fractured system. The dimensionless response variable containing a maximum withdrawal rate (or maximum drainage velocity) is called the maximum capillary number (Ca_{\max}). After the procedure employed for the critical capillary number in the previous section, the individual effect of each dimensionless group on the maximum capillary number is shown through Figures 7–9.

According to these figures, it is clear that the logarithm of dimensionless MPWR (i.e., maximum capillary number) changes linearly with “ K_f/K_m ”, Bond number, and maximum Reynolds number (Reynolds number associated with MPWR or maximum drainage velocity, “ V_{\max} ”). The logarithm of the dimensionless maximum withdrawal rate increases linearly with all of the noted dimensionless groups, except the maximum Reynolds number. Consequently, one could express the dimensionless MPWR in terms of the dimensionless parameters as follows:

$$Ca_{\max} = \frac{V_{\max} \mu_l}{\sigma} = f_2 \left(Bo, Re_{\max}, \frac{K_f}{K_m}, \text{combination of these numbers} \right)$$

$$\text{and } Re_{\max} = \frac{\rho V_{\max} D_p}{\mu} \quad (13)$$

Another point that can be concluded from Figures 7–9 is that the maximum capillary number depends upon the combination of all

three of the dimensionless parameters, namely, natural logarithms of the Bond number, “ K_f/K_m ”, and maximum Reynolds number. As a result, eq 13 is expressed in a more specific form as

$$\ln(Ca_{\max}) = a + b \ln(Bo) + c \ln(Re_{\max}) + d \ln\left(\frac{K_f}{K_m}\right) + e \left\{ \ln(Bo) \ln(Re_{\max}) \ln\left(\frac{K_f}{K_m}\right) \right\} \quad (14)$$

Table 7 contains the numerical values of the coefficients in eq 14, the standard error, and lower and upper limits of the coefficients.

Multiple Linear Regression Analysis for the Dimensionless Height. The elevation difference between G–L interface positions within the matrix and fracture is another important parameter for evaluating the performance of a CGD process. Consequently, it was considered as one of the response variables that should be predicted statistically based on the multiple linear regression analysis. As a relevant dimensionless group, the dimensionless height was defined as the ratio of model height/elevation difference between G–L interface positions within the matrix and fractures for each particular fractured system.

To perform the statistical sensitivity analysis, one could use the same procedure described earlier for CPR and MPWR. Cross-plots of dimensionless height versus different dimensionless groups (Figures 10–12) suggest the following functional form:

$$\frac{L}{\Delta h} = f_3 \left(Bo, Ca, \frac{K_f}{K_m}, \text{combination of these numbers} \right) \quad (15)$$

To present the function in a linear form regardless of increasing and decreasing trends, the natural logarithm term contributes in some of the terms. Also, the interaction term of significance in this case turned out to be a multiplication of the Bond number and logarithm of the capillary number. On the basis of this, the following model was obtained:

$$\ln\left(\frac{L}{\Delta h}\right) = a + b \ln(Ca) + c Bo + d \frac{K_f}{K_m} + e \{ Bo \ln(Ca) \} \quad \text{if } q \leq q_{cr} \quad (16)$$

$$\ln\left(\frac{L}{\Delta h}\right) = \ln\left(\frac{L}{\Delta h}\right)_{cr} \quad \text{if } q > q_{cr} \quad (17)$$

The correlation coefficients of eq 16 are presented in Table 8.

Table 7. Information Table for the Linear Regression Model of the Maximum Capillary Number ($R^2 = 0.998$; $F = 2.56186 \times 10^2$)

coefficients	numerical value	standard error	lower 95%	upper 95%
a	26.91791×10^{-2}	51.18102×10^{-2}	7.12011×10^{-2}	140.95581×10^{-2}
b	108.38952×10^{-2}	7.53903×10^{-2}	91.59080×10^{-2}	125.1883×10^{-2}
c	-2.02202×10^{-2}	15.22700×10^{-2}	-35.94903×10^{-2}	-0.90572×10^{-2}
d	5.88352×10^{-2}	6.11111×10^{-2}	7.73203×10^{-2}	1.94992×10^{-2}
e	0.78404×10^{-2}	0.19103×10^{-2}	0.36162×10^{-2}	1.2065×10^{-2}

According to eq 14, the maximum drainage velocity is present on both sides of the equation and a root solving procedure can be employed.

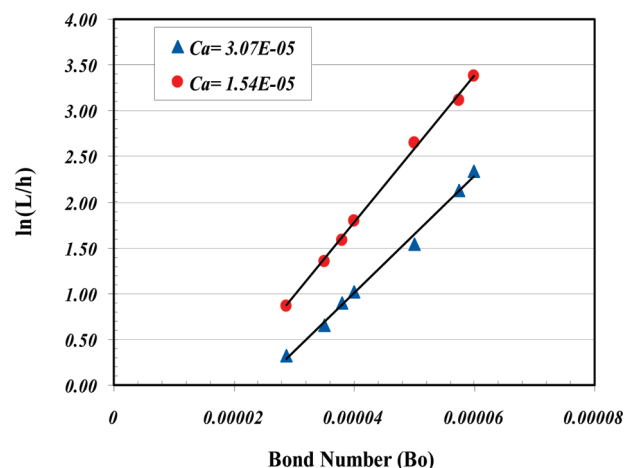
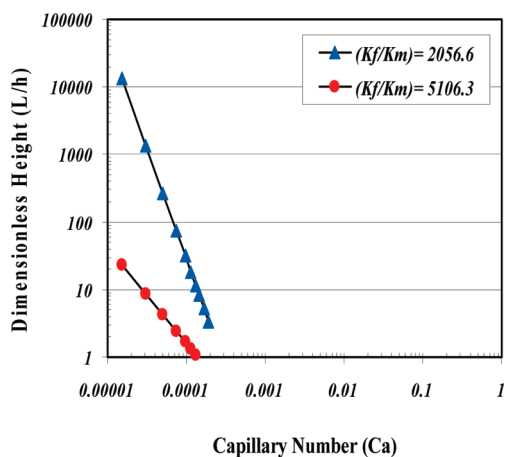


Figure 10. Dimensionless height against the capillary number, “ Ca ”, during the CGD process at various conditions.

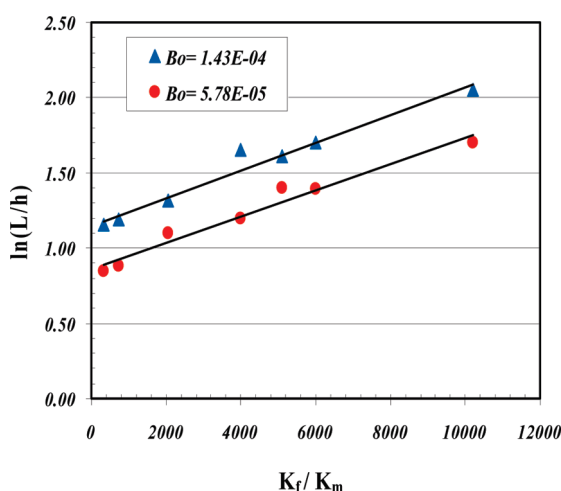


Figure 11. Effect of “ K_f/K_m ” on the natural logarithm of the dimensionless height ($\ln(L/\Delta h)$).

Multiple Linear Regression Analysis for the Recovery Factor. Because the production performance of a CGD process would be evaluated on the basis of the amount of recovered liquid with respect to the liquid initially present in place (i.e., recovery factor), it would be beneficial if one could estimate the amount of recovery factor as a function of different system characteristics. According to the same procedure presented for the other dimensionless system responses, for a fractured system analogous to the experimental schemes shown in Figure 2, one could

Figure 12. Effect of the Bond number on “ $\ln(L/\Delta h)$ ” for capillary numbers equal to 3.07×10^{-5} and 1.54×10^{-5} , respectively.

suppose the recovery factor to have a functional relationship based on the defined dimensionless groups as follows:

$$RF = f_4\left(Bo, Ca, \frac{K_f}{K_m}, \text{combination of these numbers}\right) \quad (18)$$

Performing the standard statistical procedure described before, which could result in deducing relevant cross-plots of recovery factor versus affecting dimensionless groups (Figures 13–15), the final multi-variable regressing form of the recovery factor is as follows:

$$RF = a + bCa + cBo + d\frac{K_f}{K_m} + e\left\{Ca\frac{K_f}{K_m}\right\} + f\left\{CaBo\frac{K_f}{K_m}\right\} \quad \text{if } q \leq q_{cr} \quad (19)$$

$$RF = RF_{cr} \quad \text{if } q > q_{cr} \quad (20)$$

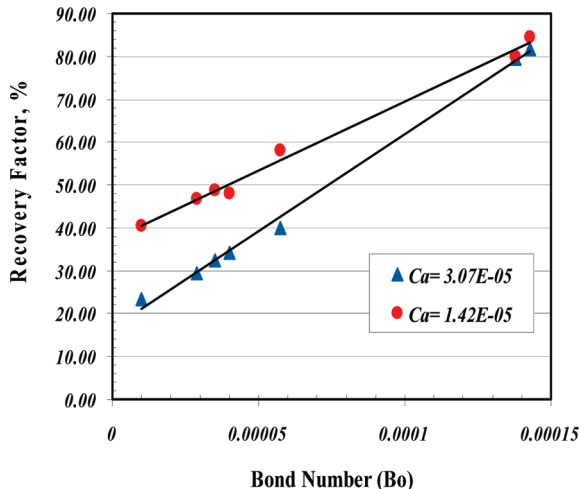
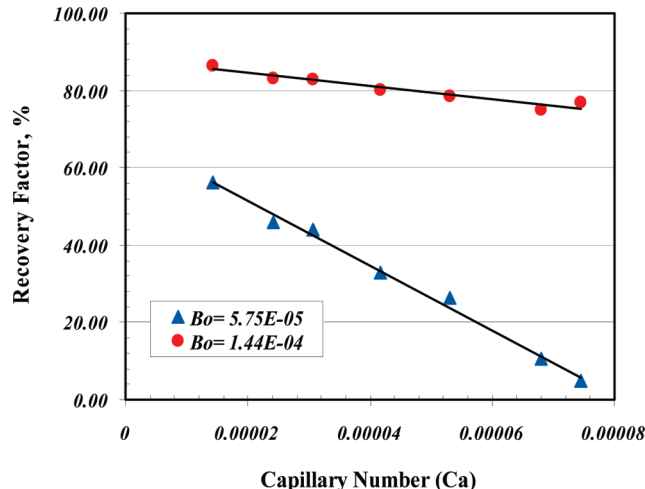
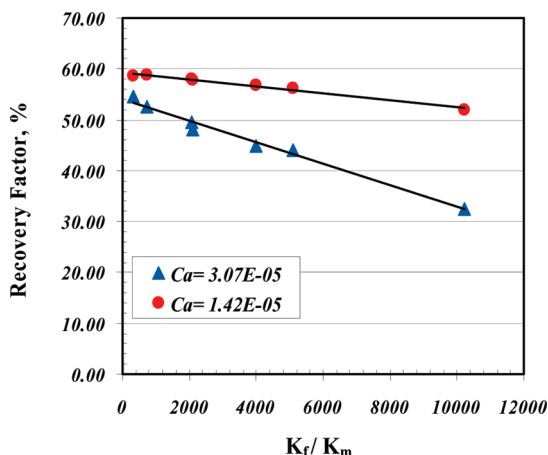
It is worthwhile to note that the product of Bond and capillary numbers as well as the interaction of all three dimensionless groups would affect the recovery factor parameter in the form of “combinatory impacts”. Curve fitting based on the regression analysis results in determining the correlation coefficients presented in Table 9.

■ ANALYSIS OF THE MULTIVARIABLE REGRESSION MODELS

The regression modeling, which is based on the assumption of validity of experimental data and, as such, the precision of preliminary design of experiment (DOE), should be checked to examine the curve fitting procedure and validity of the preliminary employed DOE. Three major validity indicators

Table 8. Information Table for the Linear Regression Model of the Dimensionless Height ($R^2 = 0.995$; $F = 6.37691 \times 10^2$)

coefficients	numerical value	standard error	lower 95%	upper 95%
a	$-371.05003 \times 10^{-2}$	125.93180×10^{-2}	$-625.19101 \times 10^{-2}$	$-116.91011 \times 10^{-2}$
b	-16.57100×10^{-2}	12.08553×10^{-2}	-40.96012×10^{-2}	-10.61850×10^{-2}
c	-16.45251×10^4	10.41173×10^3	-18.55372×10^4	-14.35131×10^4
d	9.65004×10^{-5}	2.84110×10^{-5}	3.92102×10^{-5}	15.40003×10^{-5}
e	-219.04402×10^2	10.40688×10^2	-240.04603×10^2	-198.04211×10^2

**Figure 13.** Impact of the Bond number on the production performance of the fractured porous media during CGD.**Figure 15.** Linear plot of the recovery factor versus capillary number at two different magnitudes of the Bond number.**Figure 14.** Recovery factor versus the ratio of fracture permeability/matrix permeability for two values of the capillary number.

were used to check the suitability of the multivariable linear regression analysis, namely, analysis of variance (ANOVA) tables, residual analysis, and square of residuals' analysis.^{22,23}

ANOVA Tables. The ANOVA table includes data from a standard sum of the squares of the variance analysis for regression. The relevant ANOVA table for CPR is shown in Table 10. The table includes the relevant data for each of three sources of deviation consisting of regression, residuals, and total (i.e., second column). The source of variation of each data is due to either the deviation of each predicted data from its group mean value (i.e., regression) or the deviation of each predicted value from its observed value (i.e., residuals). The sum of these two sources of deviations would

be expressed as the total source of deviations. For each of these three sources of deviations, four measures of variance (i.e., columns 3–6 in Table 10) could be described as follows. (a) Degrees of freedom (i.e., DF, third column of Table 10): For each particular regression analysis, this parameter could be determined as the number of correlation coefficients, "N", with respect to the number of regressor variables used in each particular model. The higher the degree of freedom for each particular model, the more reliable the regression model. (b) Sum of the Squares (i.e., SS; fourth column of Table 10): Summation of the squared deviations, which are predicted from the observed data, is a measure of variance for each particular regression analysis. The total SS is the summation of the squares of the residuals with the SS because of the regression. (c) Mean squares (i.e., MS; fifth column of Table 10): This column contains the sum of squares (i.e., SS) corrected for the degrees of freedom (i.e., DF). (d) F test (i.e., F; sixth column of Table 10): This is a variance-related statistical parameter that compares two models that are different from each other by one or more regressor variables to figure out if the more complex model would also be more reliable than the less complex model. If the "F" value is greater than a standard (i.e., critical) tabulated value, the more complex equation would be considered significant. By default, the significance level is set at 0.05.

According to the above descriptions, Table 10 is the ANOVA table for CPR, MPWR, dimensionless height, and recovery factor. Because F_{observed} , which is equal to 478.027 for CPR, is greater than the critical value (3.48), all of the considered parameters in multivariable linear regression analysis of CPR (i.e., critical capillary number) and their attributed effects are of great significance and, consequently, cannot be ignored to simplify the related statistical analysis.

According to the same statistical analogy, the ANOVA table could also be created for MPWR (i.e., maximum capillary

Table 9. Information Table for the Linear Regression Model of the Recovery Factor ($R^2 = 0.996$; $F = 87.68266 \times 10^1$)

coefficients	numerical value	standard error	lower 95%	upper 95%
<i>a</i>	500.75620×10^{-1}	23.25941×10^{-1}	454.33022×10^{-1}	547.18221×10^{-1}
<i>b</i>	-2.71062×10^5	86.51818×10^2	-2.88331×10^5	-2.53793×10^5
<i>c</i>	21.80125×10^4	15.58904×10^3	18.68967×10^4	24.91284×10^4
<i>d</i>	1.12903×10^{-3}	0.25604×10^{-3}	0.61805×10^{-3}	1.64103×10^{-3}
<i>e</i>	-20.33841×10^1	69.38715×10^{-1}	-21.72342×10^1	-18.95351×10^1
<i>f</i>	156.33333×10^4	59.96075×10^3	144.36510×10^4	168.30152×10^4

Table 10. ANOVA Table for CPR, MPWR, $L/\Delta h$, and RF Regression Analysis

response variable	source	DF	SS	MS	F
CPR (i.e., Ca_{cr})	regression	4	8.01002×10^{-8}	2.00021×10^{-8}	4.78027×10^2
	residual	10	4.19011×10^{-10}	4.19031×10^{-11}	
	total	14	8.05022×10^{-8}		
MPWR (i.e., Ca_{max})	regression	4	902.20501×10^{-2}	225.55101×10^{-2}	2.56186×10^2
	residual	10	8.80401×10^{-2}	0.88011×10^{-2}	
	total	14	911.00903×10^{-2}		
$L/\Delta h$	regression	4	1.93864×10^2	$4846.59102 \times 10^{-2}$	6.37691×10^2
	residual	42	319.20901×10^{-2}	7.60001×10^{-2}	
	total	46	1.97056×10^2		
RF	regression	5	266.70566×10^2	533.41130×10^1	87.68266×10^1
	residual	67	40.75898×10^1	608.34301×10^{-2}	
	total	72	270.78156×10^2		

number), as depicted in Table 10. It is clear that, because of the higher magnitude of the “F” function compared to its tabulated critical value (3.48), all of the dimensionless groups considered for the multivariable linear regression analysis of MPWR are of great importance and cannot be ignored or reduced. In addition, it is concluded that there is at least one non-zero correlation coefficient in the proposed regression model for MPWR.

The same procedure was followed to establish the ANOVA table for the other two objective functions of regression analysis, dimensionless height and recovery factor, just before gas breakthrough into the production side. Table 10 shows the strong dependency of noted objective functions to the dimensionless groups used for statistical analysis based on the high magnitude of observed “F” function compared to the tabulated critical values. In addition, this table demonstrates good accuracy of the regression analysis for both of these objective functions (dimensionless height and recovery factor).

Residual Analysis. The difference between the observed value of the dependent variable (y) and its predicted value (\hat{y}) is called the residual parameter (i.e., “e”) attributed to that particular dependent variable. Each data point has one attributed residual value based on the following definition:

$$\text{residual} = \text{observed value} - \text{predicted value} \quad (21)$$

A residual plot is a graph that shows the residual magnitudes for each particular variable on the vertical axis and the magnitudes of independent variable on the horizontal axis. If the data points in a residual plot would be randomly dispersed around the horizontal axis, that particular linear regression model is statistically appropriate; i.e., it predicts the dependent variable precisely enough compared to the actual values reported on the basis of the experimental observations; otherwise, it is recommended to use a nonlinear regression model instead of the linear model. In this section, residual plot studies were performed for all of the

statistical regression analyses to check for their validity and accuracy, besides the accuracy check performed in this study.

Residual Plots for Critical Capillary Number Regression Analysis. Panels a and b of Figure 16 are the residual plots for the critical capillary number (i.e., CPR) with respect to “ K_m/K_f ” as well as with respect to the related combined interaction component (i.e., combination of the Bond number, Reynolds number, and permeability ratio), respectively, which were included here as two samples of the residual plots for the critical capillary number. The residual data spread randomly all along the horizontal axis. In other words, the proposed linear regression is valid in terms of these two particular dependent variables. Panels a and b of Figure 17 are the comparison chart between actual (i.e., experimentally measured) and predicted values of the critical capillary number against its related interaction term (combination of the Bond number, Reynolds number, and the permeability ratio) and the Bond number (Bo), correspondingly. As depicted in this figure, there is a good compatibility between the actual and predicted values of the critical capillary number, showing reliable performance of the proposed regression analysis.

Residual Plots for Maximum Capillary Number Regression Analysis. To check the validity of the regression analysis performed for the maximum capillary number (i.e., MPWR), two related residual plots were presented as well. Panels a and b of Figure 18 show the residual plots for the maximum capillary number with respect to “ $\ln(K_f/K_m)$ ” and its values with respect to another dimensionless parameter, i.e., the related combined interaction term, respectively. Because these two residual plots did not present a certain trend with respect to the values provided in the “x axis”, it was concluded that the proposed linear regression relationship was appropriately valid for predicting the maximum capillary number using available experimental data for a system analogous to our proposed fractured systems.

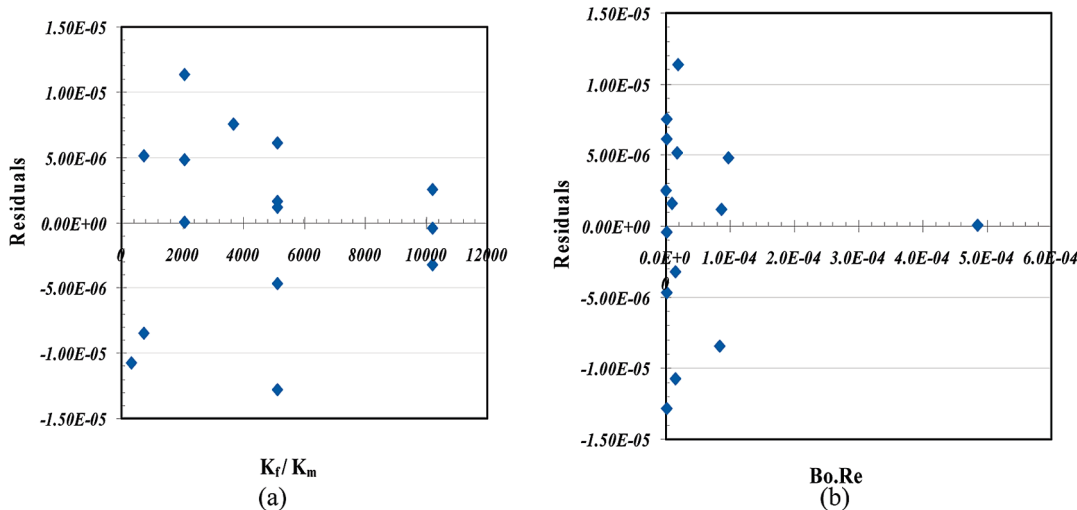


Figure 16. Residual plots for the critical capillary number. (a) Residuals of “ Ca_{cr} ” with respect to “ K_f/K_m ” dimensionless number. (b) Residuals of “ Ca_{cr} ” with respect to its related interaction component (i.e., $BoRe$).

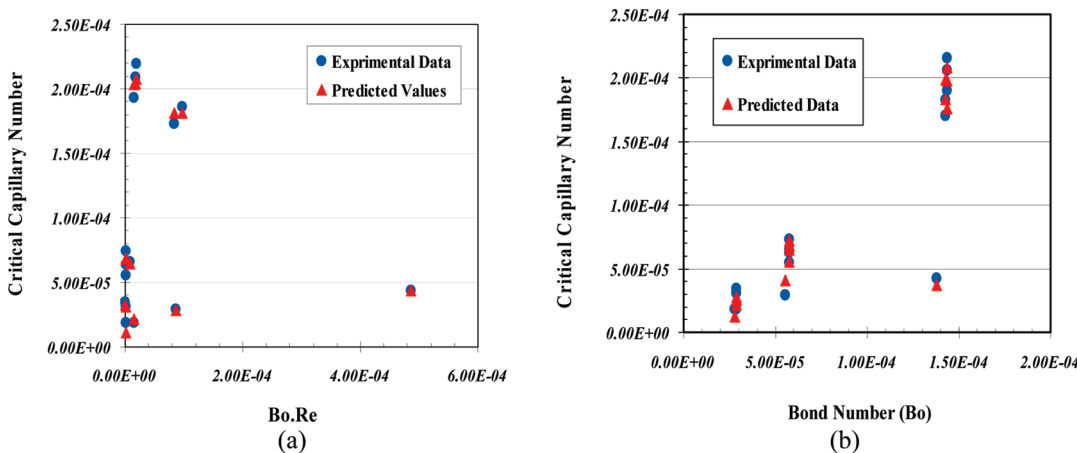


Figure 17. Comparison charts. (a) Predicted versus actual “ Ca_{cr} ” against the related interaction term. (b) Predicted versus actual “ Ca_{cr} ” against the Bond number.

A comparison between predicted and actual values of the maximum capillary number was shown in panels a and b of Figure 19 as a function of “ Ca_{max} ” and K_f/K_m . The calculated values based on the experimental data and the values predicted by the regression analysis match very well. In other words, eq 14 could predict the maximum capillary number (related to the MPWR) precisely for a system similar to the fractured models employed in our experimental approach.

Residual Plots for Dimensionless Height Regression Analysis. The two consecutive plots, panels a and b of Figure 20, show the random scattering of residual values attributed to the dimensionless height versus two of the contributing dimensionless groups based on eq 16. According to the logic provided in the paper, it would be concluded that the regression analysis presented by eq 16 accurately predict related values of dimensionless height based on the provided measurable experimental parameters for a system analogous to our fractured porous media prototypes undergoing a CGD process. As usual, this accuracy could be double-checked by comparing the actual dimensionless height

values (on the basis of the measurable experimental parameters) against its predicted values (using eq 16) in the presence of two of the contributing dimensionless groups according to eq 16 (see Figure 21). It is clear that the achieved agreement has high levels of accuracy in terms of the statistical parameters.

Residual Plots for Recovery Factor Regression Analysis. Panels a and b of Figure 22 show the residual plots of the recovery factor versus two selected contributing dimensionless groups based on eq 19, namely, a fracture permeability/matrix permeability ratio and also the combined interaction term in terms of the product of the capillary and Bond numbers, respectively. The data points are scattered randomly around the x axis, showing that the representation of the dependent variable based on that particular independent variable is valid within the range of change of the noted independent variable. In other words, the proposed linear regression analysis provided to predict the recovery factor values is precisely valid for a system analogous to our experimental fractured system. The accuracy of eq 19 to estimate the recovery factor values could also be examined by

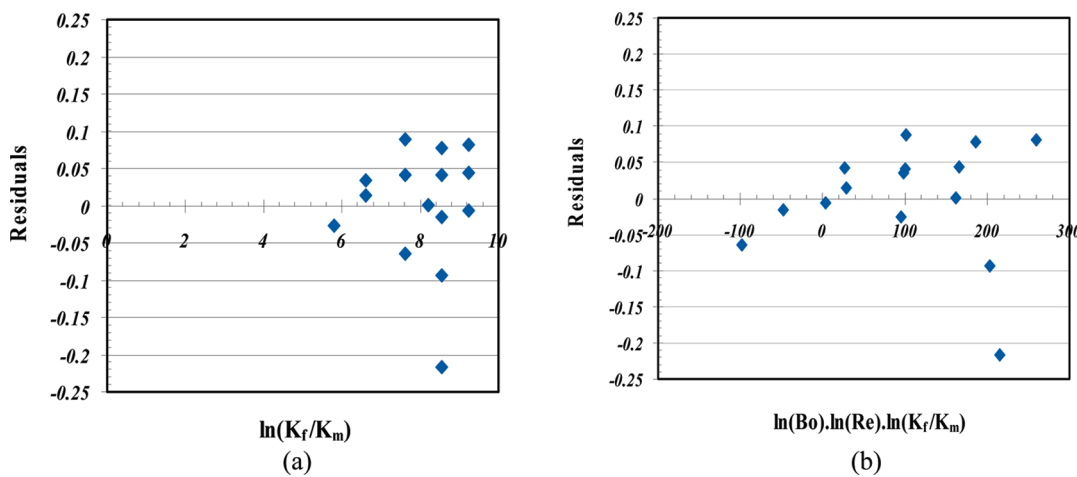


Figure 18. Residual plots for the maximum capillary number. (a) Residuals of “ $C_{a_{\max}}$ ” with respect to “ $\ln(K_f/K_m)$ ”. (b) Residuals of “ $C_{a_{\max}}$ ” with respect to its related interaction component [i.e., $\ln(Bo)\ln(Re_{\max})\ln(K_f/K_m)$].

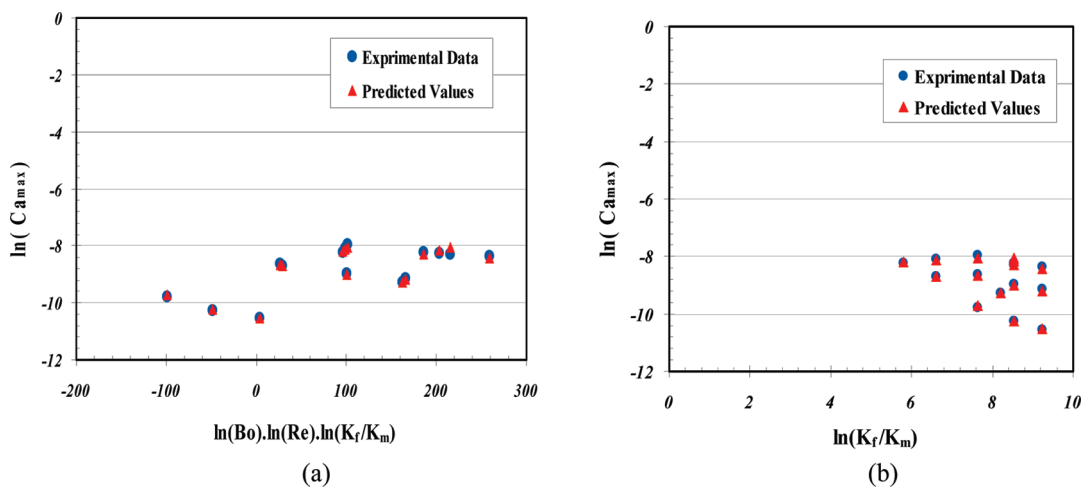


Figure 19. Comparison charts. (a) Predicted versus actual “ $C_{a_{\max}}$ ” against the related interaction term. (b) Predicted versus actual “ $C_{a_{\max}}$ ” against the term K_f/K_m .

comparing the predicted and calculated actual recovery factor values. This is the theme of panels a and b of Figure 23, in which the calculated recovery factor values (i.e., obtained from experimentally measured parameters) are in good agreement with the predicted ones using eq 19 when they were plotted against each of the independent variables, such as the capillary number and the combined interaction parameter, as in the case of this figure.

Square of Residuals' Analysis. One of the simplest methods to check the accuracy of a particular linear regression is to look at the magnitudes of squared residuals. These values for the proposed linear regressions were presented in Table 11. Our results from experimental data and linear regression analyses demonstrate reasonable compatibility between measured and predicted values. In other words, small values of residuals as well as appreciable magnitudes of the squared residual indicate that the proposed linear regression curves work well for the experimental conditions.

Validation. A real fractured medium with properties close to the properties of one of Shell's fractured carbonate reservoirs was chosen to validate the applicability of the new dimensional analysis proposed. The rock permeability was assumed as 10

millidarcy. The porosity was assumed as 32%. The height of the porous medium was assumed as 80 m. The density of the oil at the bubble-point pressure was 803.5 kg/m^3 , and the gas density was 28.4 kg/m^3 . For the fractures, permeability and effective porosity are 100 darcy and 3%, respectively. Clements and Wit²⁹ reported that the oil viscosity was 2.4 cP at bubble-point conditions. Moreover, an approximate drainage area of $200 \times 200 \text{ m}$ per well was estimated for this field. This reservoir is undergoing a gas injection process as the production starts using a pump on the ground facility. Table 12 shows the real data versus the results obtained from the regression correlations. As seen from Table 12, the proposed dimensional analysis results are in good agreement with those obtained from the real field.

On the basis of Table 12 and also the definition of CPR, MPWR, and maximum gravity drainage given by Darcy's equation, the following relationship can be written:

$$\text{CPR} < \text{maximum gravity drainage from Darcy's equation} < \text{MPWR} \quad (22)$$

In addition, the experimental data justify the above equation (see Table A1 in the Appendix).

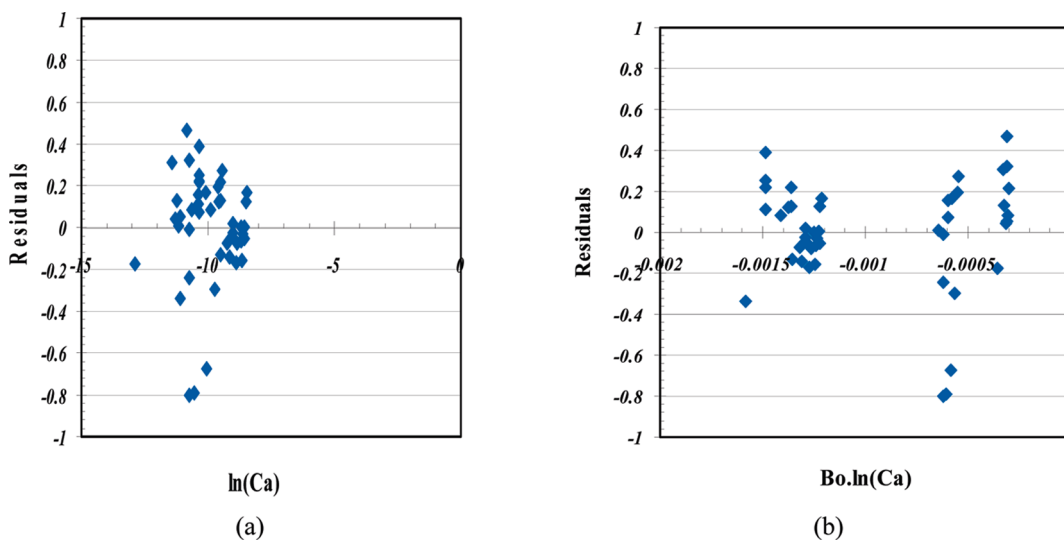


Figure 20. Residual plots for the dimensionless height. (a) Residuals of “ $L/\Delta h$ ” versus “ $\ln(Ca)$ ”. (b) Residuals of “ $L/\Delta h$ ” versus its related combined interaction term [i.e., $Bo \ln(Ca)$].

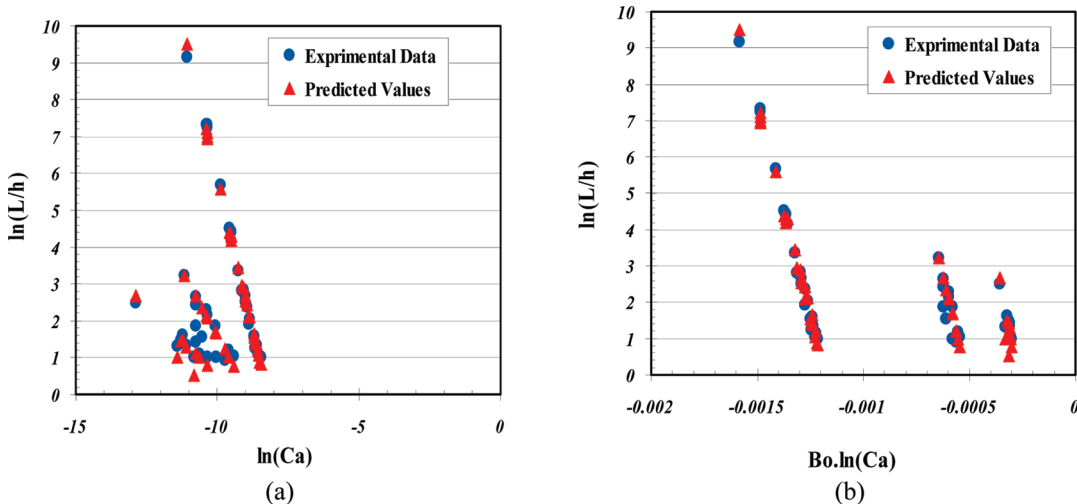


Figure 21. Comparison charts. (a) Predicted versus actual dimensionless height against the capillary number. (b) Predicted versus actual dimensionless height against its combined interaction parameter [i.e., $Bo \ln(Ca)$].

Limitations and Assumptions for the Empirical Correlations. The range of the dimensionless groups including Ca , K_f/K_m , Bo , and Re , for which the correlations of CPR, MPWR, RF, and Δh are applicable, were found to be on the order of $0-8.0 \times 10^{-5}$, $0-11.0 \times 10^3$, $0-1.5 \times 10^{-4}$, and $0-5.0$, respectively.

A number of limitations/restrictions associated with the correlations obtained in this study are listed as follows: (1) Porous medium is non-deformable; thus, it has a constant porosity. (2) No source or sink terms exist for mass. (3) Both liquid and gas phases are incompressible at the conditions (very small changes in temperature and pressure). (4) Two phases are immiscible. (5) Physical properties of fluids are constant during the experiments based on the same logic stated in the third limitation. (6) The studied case here is two-dimensional (2D) flow in porous media, although fluid flow in the gravitational direction is dominant in a vertical porous system under free fall and CGD processes, and this assumption is reasonable for all types of gravity drainage processes. (7) The correlations are valid just in the range of dimensionless numbers employed in the current

study. Ranges of dimensionless groups in oil fields are almost the same as in the experimental work. It is proven that flow in porous media is often laminar (i.e., $Re < 1$) and the Bond number is very low because of less permeable rocks in fractured reservoirs. Therefore, the Bond number is definitely in the range (stated above) for real cases. (8) Geometry of physical models does not have big effects on RF in gravity drainage; it just affects residual oil saturation slightly because geometry dictates the shape of corners and end points and no change is observed for a high capillary threshold and permeability with respect to geometry variations for the porous system. (9) There were eight different porous media with different fracture patterns, and the correlations are giving very good results with high accuracy for the porous media having these kinds of fracture configurations. Therefore, the only main limitation would be the type of fracture configuration for the fractured porous media. It should be noted, if the effective fracture permeability is known for a porous medium with unknown fracture patterns, the obtained empirical equations can help to predict the flow

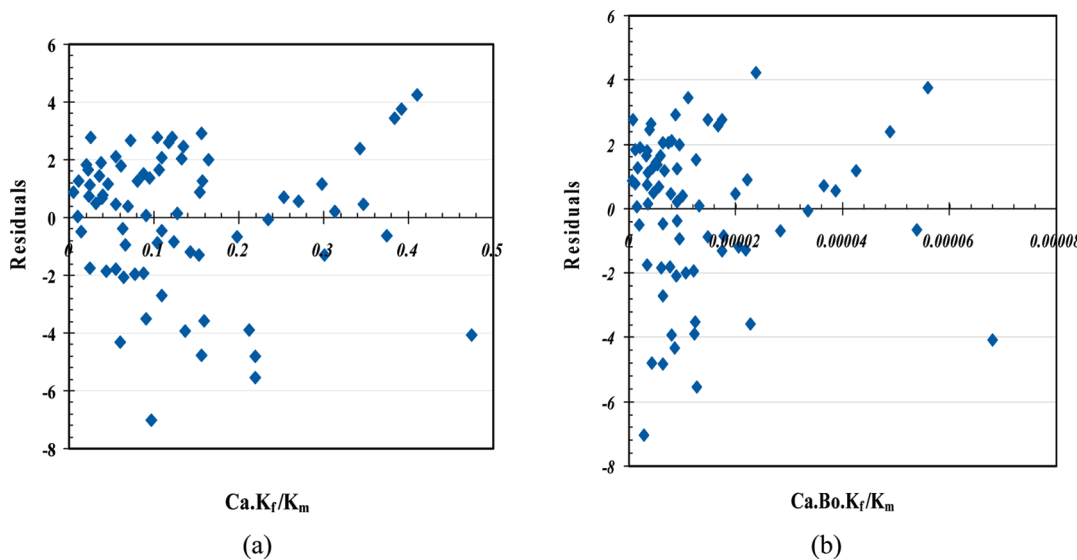


Figure 22. Residual plots for the recovery factor. (a) Residuals of RF versus the related dimensionless number, named “ CaK_f/K_m ”. (b) Residuals of RF versus the related dimensionless number (e.g., $CaBoK_f/K_m$).

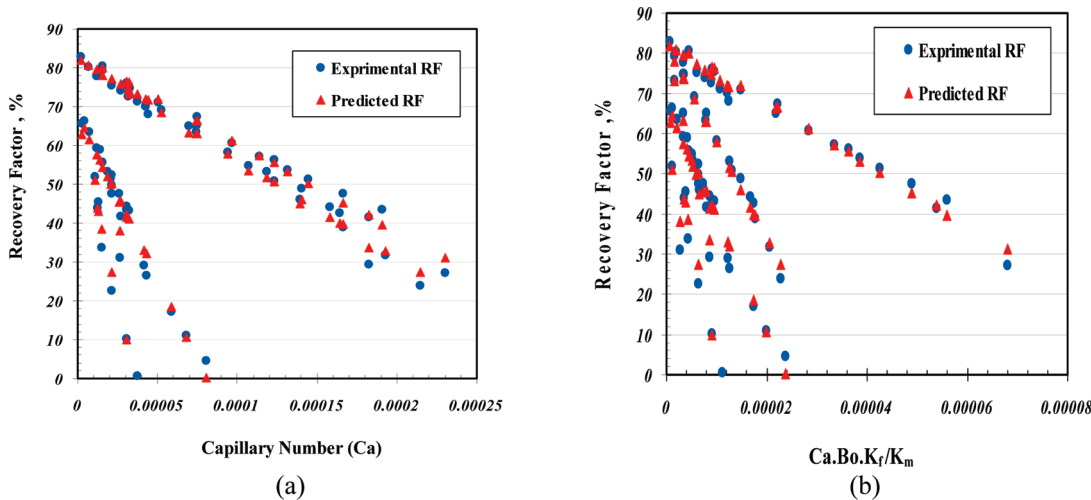


Figure 23. Comparison charts. (a) Predicted versus actual recovery factor against the capillary number. (b) Predicted versus actual recovery factor against its combined interaction term (i.e., $CaBoK_f/K_m$).

Table 11. Summary of the Statistical Linear Regressions

objective function	multiple R	R ²	standard error	number of observations
CPR	0.998	0.997	4.831×10^{-6}	19
MPWR	0.999	0.998	3.220×10^{-2}	19
($H_f - H_m$)	0.997	0.995	14.381×10^{-2}	59
recovery factor	0.998	0.996	21.312×10^{-2}	59

behavior and recovery factor of the porous system somehow (see Tables 11 and 12).

CONCLUSIONS

(1) During CGD, the elevation difference between G–L interface locations in the fracture and matrix remains constant, while liquid is pumping out of the fractured system with a constant withdrawal rate lower than the associated CPR. (2) Considering all

experimental variables to remain unchanged, the CPR is sensitive to the magnitude of liquid viscosity. (3) MPWR depends upon the storage capacity of fractures, flow properties of the matrix (i.e., permeability), and also liquid flow properties (i.e., viscosity). (4) The critical rate, maximum rate, recovery without gas breakthrough, and difference of G–L interface positions in the matrix and fracture are correlated by dimensionless numbers, such as the Bond number, capillary number, ratio of permeabilities, etc. (5) Because the experiments were carried out only over a limited range of conditions, more experiments are needed to fully validate the new dimensional analysis introduced for fractured porous media under CGD. However, these experimental results could be used to test fracture network models of gravity drainage processes. (6) Linear regression modeling presented in this paper can predict the production history and flow behavior in our fractured porous media well for a wide range of dimensionless numbers. (7) Results presented in this study suggest that the Bond and capillary numbers alone could not predict the oil production characteristics. A combination term of these

Table 12. Comparison between the Production Characteristics Obtained from the Regression Approach and Real Field

parameter	real data	data obtained from the current study
$q_{\max}^{\text{fg}} (\text{m}^3/\text{s})$	11.91	12.68
CPR (m^3/s)	not available	7.14
MPWR (m^3/s)	13.83	14.92
RF before gas breakthrough at $q = 4.2 \text{ m}^3/\text{s}$ (%)	78.9	80.1

dimensionless groups is needed to predict the oil recovery factor and system-specific rates over a wide range of petrophysical and operational properties. (8) The dimensional analysis model developed herein can match experimental and multivariable regression results for oil production from fractured porous media under CGD and has been successfully applied to actual field data in the range of the dimensionless groups stated in this paper.

■ APPENDIX: RAW DATA FOR FIVE RANDOMLY SELECTED RUNS

Table A1 presents raw data for five test runs that are conducted for the CGD processes in fractured porous media. The table contains characteristic production rates for each run and its replicates. A comparison between a particular run and the corresponding replicates for a given system shows very good repeatability of experiments.

Table A1. Raw Data for Five Test Runs Selected Randomly from Table 3

run number	model height, L (cm)	matrix glass bead type	q_{\max}^{fg} (cm^3/s)	CPR (cm^3/s)	MPWR (cm^3/s)
7			5.8	3.0	6.2
replicate 1	55	BT3	5.6	3.2	6.0
replicate 2			5.5	3.1	6.1
10			2.9	0.9	3.9
replicate 1	28	BT3	2.7	0.8	3.7
replicate 2			2.7	0.7	3.8
11			3.3	1.2	4.4
replicate 1	40	BT3	3.5	0.9	4.3
replicate 2			3.6	1.2	4.5
12			3.9	1.4	5.3
replicate 1	55	BT4	4.1	1.5	5.0
replicate 2			4.0	1.3	5.0
18			3.8	3.5	5.1
replicate 1	55	BT2	3.6	3.3	4.8
replicate 2			3.7	3.4	4.8

■ AUTHOR INFORMATION

Corresponding Author

*E-mail: szendehb@uwaterloo.ca.

■ ACKNOWLEDGMENT

The authors gratefully acknowledge financial support for this research provided by the Natural Sciences and Engineering Research Council (NSERC) of Canada.

■ NOMENCLATURE

Acronyms

- ANOVA = analysis of variance
- CGD = controlled gravity drainage
- CMC = carboxy methyl cellulose
- CPR = critical pumping rate
- DF = degree of freedom
- DOE = design of experiment
- FFGD = free fall gravity drainage
- G–L = gas–liquid
- IFT = interfacial tension
- MPWR = maximum possible withdrawal rate
- MS = mean squares
- NFR = naturally fractured reservoir
- SS = sum of the squares

Variables

- Ar = Archimedes number ($gL^3\rho_l^2)/\mu_l^2$
- a, \dots, g = coefficients of the linear regression equations
- Bo = Bond number ($\Delta\rho g K_m)/\sigma$
- b = fracture aperture (m)
- Ca_{cr} = critical capillary number ($V_{\text{cr}}\mu)/\sigma$
- D_p = bead particle diameter (m)
- e = error value in eqs 5–7
- Fr_{PM} = Froude number in porous media, $V^2/(g(K_m)^{1/2})$
- g = gravitational acceleration (m/s^2)
- $H(t)$ = gas–liquid interface position measured from the top of the model (m)
- H_m = gas–liquid interface position in the matrix measured from the top of the model (m)
- H_f = gas–liquid interface position in the fracture measured from the top of the model (m)
- h_c = capillary height (m)
- K = intrinsic permeability (darcy or m^2)
- K_f = intrinsic permeability of the fracture (darcy or m^2)
- K_m = permeability of the matrix in the model (darcy or m^2)
- K_e = total effective permeability (darcy or m^2)
- L = model height (m)
- L_f = fracture height (m)
- PV = pore volume (m^3)
- q_{cr} = critical pumping rate (m^3/s)
- q_{\max} = maximum pumping rate (m^3/s)
- q = liquid flow rate during FFGD or CGD (m^3/s)
- Re_{cr} = critical Reynolds number ($\rho V_{\text{cr}} D_p)/\mu_l$
- RF = recovery factor
- S = liquid saturation
- t = time (s)
- V = darcy velocity (m/s)
- W = width of the model (m)
- x_i = regression variables in eqs 5–7
- y = system response in eqs 5–7

Greek Letters

- β_i = regression coefficients in eqs 5–7
- ϕ_e = total effective porosity of the model
- ϕ_f = fracture porosity, volume of the fracture over the total bulk volume of the model
- ϕ_m = matrix porosity, pore volume of the matrix over the bulk volume of the matrix
- μ = dynamic viscosity (kg m s^{-1} or cP)
- Δ = difference operator

ρ = density of fluid (kg/m^3)

σ = gas–liquid surface tension (N/m)

Subscripts

c = capillary

cr = critical

e = effective

f = fracture

i = number of test runs

m = matrix

max = maximum

min = minimum

or = residual oil

P = pore

PM = porous media

Superscripts

fg = free fall gravity drainage

■ REFERENCES

- (1) Saidi, A. M. *Reservoir Engineering of Fractured Reservoirs*; Total Edition Press: Paris, France, 1987.
- (2) van Golf-Racht, T. D. *Fundamentals of Fractured Reservoir Engineering*; Elsevier: Amsterdam, The Netherlands, 1982.
- (3) Dullien, F. A. L. *Porous Media, Fluid Transport and Pore Structure*, 2ed.; Academic Press: New York, 1992.
- (4) Gharbi, R.; Peters, E.; Elkamel, A. Scaling miscible fluid displacement in porous media. *Energy Fuels* **1988**, *12*, 801–814.
- (5) Gharbi, R. Dimensionally scaled miscible displacement in heterogeneous permeable media. *Transp. Porous Media* **2002**, *48*, 271–290.
- (6) Bear, J. *Dynamics of Fluids in Porous Media*; Elsevier: Amsterdam, The Netherlands, 1972; pp 665–727.
- (7) Leverett, M. C.; Lewis, W. B.; True, M. E. Dimensional-model studies of oil-field behaviour. *Trans. AIME* **1942**, *146*, 175–193.
- (8) Engelberts, W. F.; Klinkenberg, L. J. Laboratory experiments on the displacement of oil by water from packs of granular materials. *Proceedings of the Third World Petroleum Congress*; The Hague, The Netherlands, 1951; Section II, pp 544–554.
- (9) Croes, G. A.; Schwarz, N. Dimensionally scaled experiments and the theories on the water-drive process. *Trans. AIME* **1955**, *204*, 35–42.
- (10) Grattoni, C. A.; Jing, X. D.; Dawe, R. A. Dimensionless groups for three-phase gravity drainage flow in porous media. *J. Pet. Sci. Eng.* **2001**, *29*, 53–65.
- (11) Kulkarni, M. M.; Rao, D. N. Characterization of operative mechanisms in gravity drainage field projects through dimensionless analysis. *Proceedings of the Society of Petroleum Engineers (SPE) Annual Technical Conference and Exhibition*; San Antonio, TX, Sept 2006; SPE 103230.
- (12) Wood, D. J.; Lake, L. W.; Johns, R. T. A screening model for CO₂ flooding and storage in Gulf Coast reservoirs based on dimensionless groups. *Proceedings of the Society of Petroleum Engineers (SPE)/Department of Energy (DOE) Symposium improved oil recovery*; Tulsa, OK, April 2006; SPE 10021.
- (13) Offeringa, J.; van der Poel, C. Displacement of oil from porous media by miscible liquids. *Trans. AIME* **1954**, *201*, 310–315.
- (14) Rapoport, L. A.; Leas, W. J. Properties of linear waterfloods. *Trans. AIME* **1953**, *198*, 139–148.
- (15) Rapoport, L. A. Scaling laws for use in design and operation of water–oil flow model. *Trans. AIME* **1955**, *204*, 143–150.
- (16) Geertsma, J.; Croes, G. A.; Schwarz, N. Theory of dimensionally scaled models of petroleum reservoirs. *Trans. AIME* **1956**, *207*, 118–127.
- (17) Craig, F. F.; Sanderlin, J. L.; Moore, D. W.; Geffen, T. M. A laboratory study of gravity segregation in frontal drives. *Trans. AIME* **1957**, *210*, 275–282.
- (18) Perkins, F. M.; Collins, R. E. Scaling laws for laboratory flow models of oil reservoirs. *Trans. AIME* **1960**, *219*, 383–385.
- (19) van Daalen, F.; Van Domselaar, H. R. Scaled fluid-flow models with geometry differing from that of prototype. *SPE J.* **1972**, *12*, 220–228.
- (20) Rostami, B.; Kharrat, R.; Pooladi-Darvish, M.; Ghotbi, C. Identification of fluid dynamics in forced gravity drainage using dimensionless groups. *Transp. Porous Media* **2010**, *83*, 725–740.
- (21) Zendehboudi, S. Investigation of gravity drainage in fractured porous media. Ph.D. Dissertation, The University of Waterloo, Waterloo, Ontario, Canada, Sept 2010; p 249.
- (22) Montgomery, D. C.; Runger, G. C. *Applied Statistics and Probability for Engineers, Student Solutions Manual*; John Wiley and Sons: New York, 2006.
- (23) Montgomery, D. C. *Introduction to Statistical Quality Control*; John Wiley and Sons: New York, 2008.
- (24) Zendehboudi, S.; Chatzis, I. Experimental study of controlled gravity drainage in fractured porous media. *J. Can. Pet. Technol.* **2011**, *50* (2), 56–71.
- (25) Zendehboudi, S.; Chatzis, I.; Dusseault, M. B.; Shafiei, A. Empirical modeling of gravity drainage in fractured porous media. *Energy Fuels* **2011**, *25* (3), 1229–1241.
- (26) Zendehboudi, S.; Rezaei, N.; Chatzis, I. Effects of fracture properties on gravity drainage processes. *J. Porous Media* **2011**, manuscript accepted for publication.
- (27) Firoozabadi, A. *Research Program on Fractured Petroleum Reservoirs*; Department of Energy (DOE): Washington, D.C., April 1994; DE-FG22-93BC14875.
- (28) Sahimi, M. *Flow and Transport in Porous Media and Fractured Rock*, 2nd ed.; Elsevier: Amsterdam, The Netherlands, 1995.
- (29) Clemens, T.; Wit, K. The effect of fracture spacing on gas/oil gravity drainage in naturally fractured reservoirs. *Proceedings of the Society of Petroleum Engineers (SPE) Annual Technical Conference and Exhibition*; New Orleans, LA, Oct 2001; SPE 71507.
- (30) Zendehboudi, S.; Chatzis, I.; Shafiei, A.; Dusseault, M. B. Numerical simulation of gravity drainage in porous media. *J. Porous Media* **2011**, manuscript accepted for publication.
- (31) Gary, G. F. *Essentials of Multiphase Flow and Transport in Porous Media*; John Wiley and Sons: New York, 2008.